Journal of Hydrology 668 (2026) 134989

Contents lists available at ScienceDirect

Journal of Hydrology

journal homepage: www.elsevier.com/locate/jhydrol

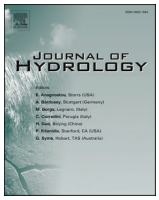

Recharge elevation, residence time and renewability of groundwater in the Upper Awash valley, Ethiopia: Applying environmental tracers in a highly populated volcanic basin

W. George Darling [a,*], James P.R. Sorensen [a], Tilahun Azagegn [b], Behailu Birhanu [b], Seifu Kebede [c], Daren C. Gooddy [d], Koos Groen [e], Richard G. Taylor [f], Alan M. MacDonald [g]

[a] British Geological Survey, Maclean Building, Wallingford OX10 8BB, UK
[b] School of Earth Science, Addis Ababa University, PO Box 1176, Addis Ababa, Ethiopia
[c] Centre for Water and Environment, North-West University, Potchefstroom Campus, Private Bag X6001, Potchefstroom, South Africa
[d] UK Centre for Ecology and Hydrology, Maclean Building, Wallingford OX10 8BB, UK
[e] Acacia Water BV, Van Hogendorpplein 4, 2805 BM Gouda, Netherlands
[f] Department of Geography, University College London, London WC1E 6BT, UK
[g] British Geological Survey, Lyell Centre, Research Avenue South, Edinburgh EH14 4AP, UK

ARTICLE INFO

This manuscript was handled by Y Huang, Editor-in-Chief

Keywords:
Groundwater
Isotopes
CFCs and SF_6
Water quality

ABSTRACT

The Upper Awash Basin in Ethiopia, which contains the rapidly-expanding national capital Addis Ababa, is being increasingly impacted by groundwater abstraction, leading to falling water levels in many areas. Groundwater management is impaired by the lack of consensus over detailed (hydro)geological characterisation of the complex volcanic aquifers that underlie this high-relief basin. Here we use an empirical study based on environmental tracers (isotopes, trace gases and hydrochemistry) measured on 40 groundwater samples collected from a selection of borehole sites, to explore the hydrogeological functioning of the basin The stable isotopes $\delta^{18}O$ and $\delta^{2}H$ provide information on likely recharge elevations (1900–3500 m above sea level) and extent to which surface waters are contributing to recharge (45% of sites sampled). The trace gases CFCs and SF_6 show that proportions of modern water are generally $< 10\%$, but ^{14}C indicates that the groundwater storage currently critical for buffering change is in most cases of the order of hundreds rather than thousands of years old, and therefore may be vulnerable to comparatively rapid modification. With little evidence for significant variation in hydrogeochemical changes with depth across individual wellfields, we conclude that recharge is usually derived locally, though indications of longer flow paths exist in some locations, principally around the town of Mojo. Hydrochemistry shows that inorganic groundwater quality remains good at present, despite the existence of some poor-quality surface waters. The methodology of this study could be applied in other high-relief basins reliant on groundwater, to characterise vulnerability to abstraction where a detailed geological model and long-term monitoring are absent.

1. Introduction

With the widespread use of data from the GRACE satellites (Rodell et al. 2018), recent collation of in-situ groundwater level data (Jasechko et al. 2024) and projections from climate change, there is renewed scrutiny on the sustainability of current and future groundwater development. Although regional inferences can be made from GRACE (e.g. Scanlon et al 2022), information on the risks of over-exploitation from individual aquifers or cities relies much more heavily on long-term in-situ monitoring data coupled with detailed geological and hydrogeological data collection and conceptualisation (MacDonald et al., 2021). However, such information is often not widely available for cities, and to build up such data would be costly and take decades to generate the water level data required to explore trends and renewability. One such example is the Upper Awash Basin (UAB) in Ethiopia which relies heavily on groundwater to sustain urban demands from Addis Ababa and competing industrial and agricultural requirements across its four topographic catchments. Addis Ababa is the capital of

* Corresponding author.
E-mail address: wgd@bgs.ac.uk (W.G. Darling).

https://doi.org/10.1016/j.jhydrol.2026.134989
Received 20 June 2024; Received in revised form 3 March 2025; Accepted 16 January 2026
Available online 23 January 2026

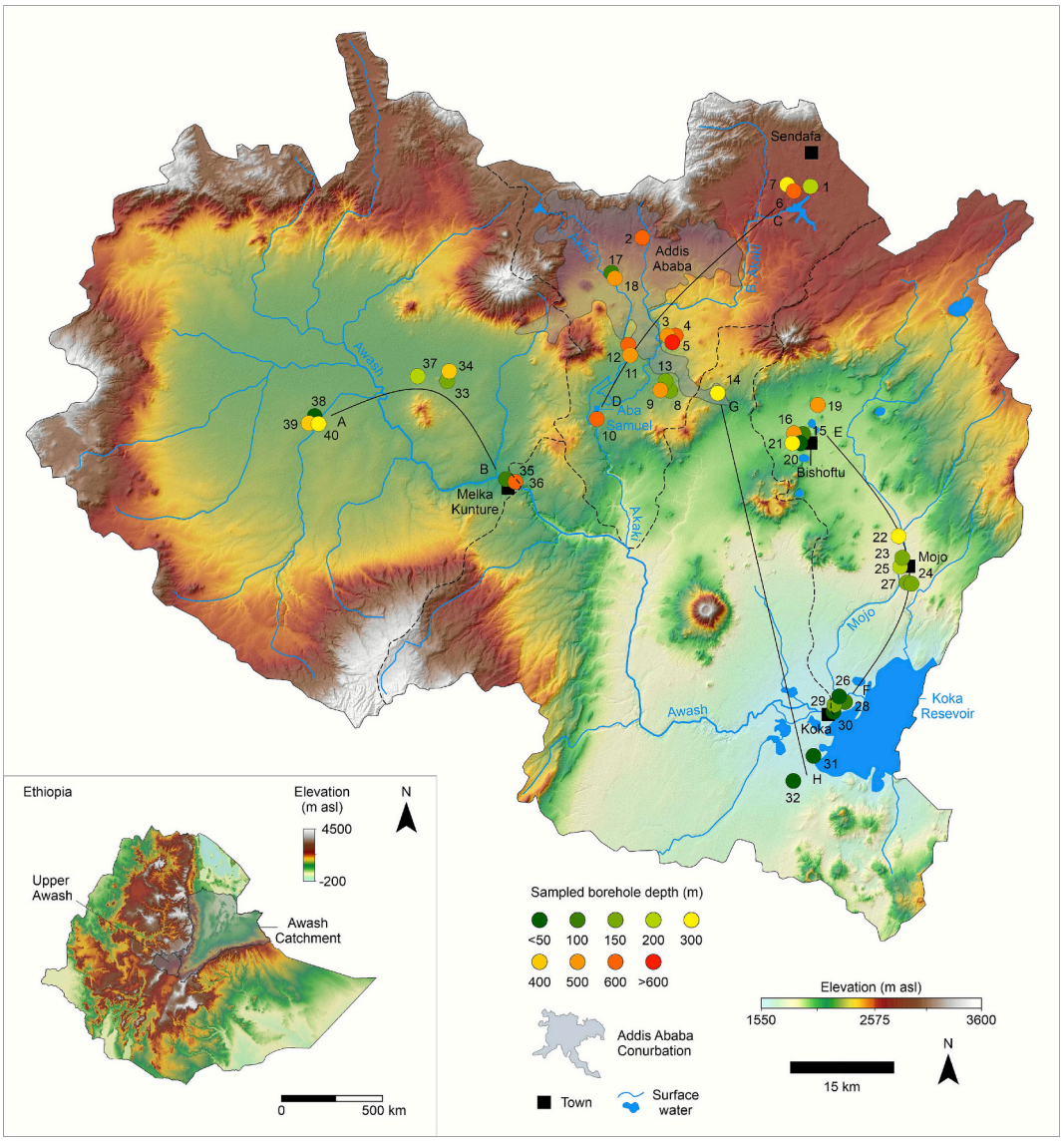

Fig. 1. Topographic map of the Upper Awash basin and its location within Ethiopia, showing the surface water catchments Melka Kunture (MK), Akaki, Mojo and Koka, with the location of Addis Ababa and other major settlements. A borehole transect line is shown for each of the catchments (A-B, C-D, E-F, G-H).

Ethiopia with a rapidly rising population of currently around 6 million people. Like many fast-growing cities in the world, domestic and industrial water demand has become a pressing issue (Scanlon et al. 2023). While surface waters from the Awash and its tributaries can satisfy some of this demand, groundwater is becoming a major contributor (Muleta and Abate, 2021). Groundwater is also increasingly relied on for horticultural exports, including the flourishing floriculture industry, with Ethiopia now the sixth largest producer and exporter of flowers globally (Gelaye 2023). In a context of immature water governance and rapidly falling water levels (Hailu et al., 2023), together with a recent tendency for deeper drilling, there is an urgent need to develop a better understanding of the hydrology of the basin.

The heterogeneous volcanic nature of the terrain adds an extra layer of challenge to characterising groundwater flow. Groundwater can potentially take many routes from recharge to discharge, thereby increasing the uncertainty regarding the area(s) of infiltration, amount of storage in the system, and possible issues affecting water quality such as sewage or industrial contamination. Whereas in a relatively flat-lying sedimentary basin a few well-characterised boreholes along a probable flowline may provide sufficient physical and chemical information to understand the individual aquifers, this is rarely an option in a complex volcanic aquifer system such as found in the UAB. Therefore, the objective of this studyis to circumvent at least some of the deficit in physical characterisation, and indeed detailed geological knowledge, by using environmental tracers to elucidate pathways and processes occurring in the subsurface, and to relate these where feasible to groundwater–surface water interaction. Stable isotopes, trace gases, radioisotopes and inorganic hydrochemistry have been measured on groundwater samples collected from a range of depths to provide information on origin, evolution and residence time, in order to arrive at an improved knowledge of how this aquifer system currently functions. Such information is critical for managing aquifers under increasing pressure and balancing the opportunity for development with the risks from overexploitation. In using tracers in this way, the study provides a blueprint for developing a relatively rapid and low cost method for greater insight into the groundwater dimension of other water-stressed cities in high-relief basins across the world..

2. Background

2.1. The basin

The UAB occupies a prominent embayment on the west side of the Main Ethiopian rift valley (MER), where the river has exploited a breach in the rift wall associated with the Yerer–Tulu Welel volcanic lineation (YTVL, Adhana, 2014) and the transition between the central and northern sectors of the MER (Bonini et al., 2005). With an area of 11,000 km^2, the UAB covers a zone extending from the Central Highlands, locally reaching ~ 3500 m asl (above sea level), to the relative lowlands of the MER lying at ~ 1600 m asl in this area (Fig. 1). The basin is characterised by locally rugged topography and consequently steep hydraulic gradients exist in parts of the basin (Muleta and Abate, 2021). We define the outlet of the catchment as Koka Dam; while the hydrograph separation-derived baseflow index (BFI, Gustard et al., 1992) here is only 0.34, implying a large relative surface runoff component, in the centre of the basin at Melka Kunture it rises to 0.65 (Tafesse, 2018), indicating that groundwater is playing a more significant role at higher elevations (see also Tadesse et al., 2023). The topographic boundary of the UAB shown in Fig. 1 probably does not fully coincide with the groundwater catchment, which is likely to include part of two sub-catchments of the Abbay (Blue Nile) basin to the north (Yitbarek et al., 2012; Azagegn et al., 2015; Berehanu et al., 2017; Tadesse et al., 2023).

Mean annual air temperature across the basin varies from 15°C at Sendafa (2500 m asl) to 24°C at Koka (1550 m asl). Mean annual rainfall on the basin averages 1030 mm (Daba et al., 2020) and falls mainly in July–August, the only months when rainfall exceeds potential evapotranspiration (PET), which varies annually from 1800 mm in the highlands to 2300 mm in the lowlands (Chan et al., 2020). The catchment therefore has to shed an average of ~ 11,000 million m^3 per year by a combination of ET, surface and subsurface flow. Tolera et al. (2018) estimated that ET accounted for some 6000 million m^3, whereas the Awash flows into Koka reservoir at a mean annual rate of 1540 million m^3 (Berhanu and Bisrat, 2020). Current abstraction for urban water supply at an estimated 250 million m^3 is small in comparison, and much may be recycled. But although there is considerable uncertainty involved in some of these figures, they imply the existence of a substantial flow of groundwater out of the Upper Awash catchment.

For the purposes of this study, the UAB has been divided into four topographic sub-catchments (after Birhanu et al., 2021): Melka Kunture (hereafter MK), Akaki, Mojo and Koka (Fig. 1). The last named includes the course of the Awash between Melka and the entry to the Koka reservoir, where evaporation and irrigation returns lead to high-TDS water. The reason for this subdivision is to facilitate comparison between catchment areas with differing topography and population density.

2.2. Previous research

Several hydrogeochemically-based studies have investigated the UAB, either by sub-catchment (Demlie et al., 2007; Demlie et al., 2008; Demlie, 2015), whole catchment (Yitbarek et al., 2012) or as part of the wider Awash river system (Ayenew et al., 2008). Others have focused on more specific areas of the rift flanks and floor (Kebede et al., 2008; Kebede et al., 2010; Bretzler et al., 2011). All have some implications for the current study.

In the Akaki sub-catchment (Fig. 1), which includes the whole of Addis Ababa, Demlie et al. (2007) noted a geology-related trend from Ca-HCO_3 waters in the north to Mg-CO_3 waters in the south, with some anionic 'overprinting' by Cl, SO_4 and NO_3 from pollution, and an input of Na-HCO_3 thermal water from the Filwoha Graben, which lies along a WSW–ENE fault system beneath central Addis Ababa. Demlie et al. (2008) added to this by interpreting tritium (^3H) measurements to suggest that most groundwaters had a recent component. A further estimation of an 18% recharge rate was derived from a combination of soil water and chloride mass balances (Demlie, 2015).

In the UAB as a whole, Yitbarek et al. (2012) interpreted their hydrogeochemical results in terms of an upper basaltic aquifer with low mineralisation, and a lower basaltic aquifer (>250 m) with moderate mineralisation but more-depleted stable isotopes. Again, a localised input of thermal water beneath Addis Ababa was identified.

There has been rather little focus on trace elements in the UAB. Soil and groundwater in the Akaki catchment were measured for heavy metals by Demlie and Wohnlich (2006), who found some high concentrations in the Akaki catchment, while Aschale et al. (2021) investigated the source of potentially toxic elements in the surface waters of the Little Akaki river system in and around Addis Ababa.

In their transect of sites from Addis Ababa to the rift floor, Kebede et al. (2008) stressed the importance of individual rock types in governing major-element water quality, but also raised the question of whether deep, isotopically-depleted groundwaters were recharged at higher elevation, or under past colder climatic conditions. This was considered further in Kebede et al. (2010), but without drawing a firm conclusion in the absence of sufficient residence time information. Finally, Bretzler et al. (2011) investigated the feasibility of ^{14}C groundwater dating in the rift setting. Although the study was mainly concerned with establishing the provenance of rift floor groundwaters rather than characterising the UAB, four sites from the UAB were included, which gave results interpreted as mean residence times < 2000 yrs.

While all the above studies have contributed to a better understanding of one or more of the four UAB sub-catchments, certain aspects in particular remain in need of improved characterisation: source and elevation of recharge, groundwater residence time and the nature of any relationship between shallow and deep groundwater. These are the main focus of the present study.

3. Methods

In addition to inorganic hydrochemistry, a standard component of such investigations, the following more specialised environmental tracers were used as part of this study.

3.1. Stable O and H isotopes

The stable isotope parameters $\delta^{18}O$ and $\delta^{2}H$ are frequently used as water process tracers (Clark and Fritz, 1997). In a typical resource study, they are called upon to establish the likely elevation(s) of recharge, and also the possibility of evaporation having affected the isotope ratio owing to surface exposure at some point in the sample's history (Gat, 1971). Less often they can be used as potential corroboration of 'palaeowater' status, i.e. water that has been recharged under a past colder climate (e.g. Edmunds, 2008).

The application of O and H stable isotopes requires the establishment of an isotopic 'lapse rate' (i.e. change in isotopic composition with elevation) for groundwater recharge in the area concerned. The gradient of this change may be inferred from a temperature lapse rate, or estimated by comparison with other studies in the region. The lapse rate for rainfall $\delta^{18}O$ where measured in Ethiopia is around –0.12‰/100 m in the Blue Nile basin and –0.11‰/100 m in the Bale Mountains (Lemma et al., 2020). Such rates are typical of African montane climates (e.g. Gonfiantini et al. 2001; McKenzie et al., 2010). Since groundwater is derived from rainfall, it is reasonable to assume that groundwater lapse rates will be similar in gradient: this, for example, has been found to be the case for Kilimanjaro (McKenzie et al., 2010; Otte et al., 2017). The intercept, however, may be different because of processes which may modify the isotopic content of recharge compared to that of weighted mean rainfall such as seasonality and intensity (Gat, 1971; Thaw et al., 2025). To find the intercept requires the isotope value of recharge considered to be local in elevation, which can be a challenge in a

Table 1
Location of sites, borehole information and field measurements for the sampling of sites in the Upper Awash basin.

Site	Site name	Date	Lat	Long	BH elev	BH depth	Temp	SEC	pH	Alk	DO
	Catchment		**°N**	**°E**	**m asl**	**m**	**°C**	**µS/cm**		**mg/L**	**mg/L**
	Akaki										
1	LLA4	07 May 2019	9.095	38.991	2463	181	25.6	435	7.8	234	0.1
2	NPPW	07 May 2019	9.028	38.770	2402	550	23.2	498	7.0	234	1.5
3	Heineken 1	08 May 2019	8.900	38.807	2180	505	35.3[c]	729	8.0	374	0.1
4	Heineken 2	08 May 2019	8.900	38.807	2188	466	32.9[c]	724	7.8	390	0.3
5	Heineken 5	08 May 2019	8.900	38.807	2174	780	61.5	1466	7.8	552	0.3
6	LLA3	08 May 2019	9.092	38.967	2469	590	28.1	465	7.9	244	<0.1
7	ZEBYM	08 May 2019	9.098	38.961	2471	230	21.8	295	7.1	162	1.1
8	Akaki AK18	09 May 2019	8.831	38.802	2065	140	24.9	503	7.5	280	5.8
9	Akaki AK22R	09 May 2019	8.830	38.797	2064	462	24.4	512	7.5	282	4.9
10	BH 18 Aba Samuel	09 May 2019	8.790	38.710	2043	503	36.0	465	7.1	289	1.5
11	Akaki AK4B	09 May 2019	8.874	38.754	2062	480	25.3	624	7.3	335	2.5
12	Salo St George SG-PW-01/16	10 May 2019	8.888	38.751	2087	537	39.3	587	7.9	293	0.6
13	Akaki AK20[a]	10 May 2019	8.840	38.800	2068	149	24.5	576	7.7	290	6.4
17	CCM Church	12 May 2019	8.982	38.729	2289	92	25.9	525	7.1	282	6.2
18	Mekanisa[a]	12 May 2019	8.975	38.734	2229	463	66.3	687	9.3	199	2.5
	Mojo										
15	MKC	11 May 2019	8.769	38.980	1897	80	21.2	742	7.3	406	3.9
16	Bishoftu 500	11 May 2019	8.769	38.979	1884	500	32.7	568	7.7	385	0.1
19	Shimbara BH11	13 May 2019	8.809	39.001	1892	500[b]	29.9	455	7.3	302	1.4
20	Bishoftu 46	13 May 2019	8.769	38.979	1891	46	21.6	632	7.0	365	2.7
21	Bishoftu 200	13 May 2019	8.769	38.978	1891	206	26.2	547	7.6	360	0.2
22	Mojo BH10	14 May 2019	8.637	39.108	1799	224	33.9	644	7.2	400	1.7
23	Mojo BH6	14 May 2019	8.608	39.112	1761	150	27.9	630	7.2	401	1.1
24	Mojo BH9	14 May 2019	8.574	39.125	1781	130[b]	28.8	508	7.2	324	3.0
25	Tafi Abo	15 May 2019	8.597	39.110	1763	200[b]	32.4	703	7.2	418	0.6
26	Dummen 48[a]	15 May 2019	8.420	39.029	1605	48	37.8	1575	8.2	622	3.9
27	Mojo BH8	15 May 2019	8.576	39.119	1763	134	28.6	528	7.2	317	2.7
28	Dummen 100[a]	16 May 2019	8.420	39.031	1599	100	68.1	2611	8.0	966	1.7
29	Florensis BH1	16 May 2019	8.416	39.023	1594	110	43.4	1543	8.2	756	0.5
30	Syngenta 40	16 May 2019	8.409	39.022	1590	40	33.5	1989	8.2	1056	0.6
	Melka Kunture										
33	Tefki Old	17 May 2019	8.850	38.513	2058	120	24.1	648	7.3	256	0.4
34	Tefki New	17 May 2019	8.851	38.515	2056	315	26.4	488	7.3	258	0.4
35	Minaye Flower Farm	18 May 2019	8.712	38.590	2000	52	26.9	523	7.1	317	1.8
36	Artesian near Minaye	18 May 2019	8.708	38.603	1997	550[b]	30.2	545	7.2	328	1.4
37	Bonday	18 May 2019	8.846	38.473	2065	200[b]	22.4	621	7.1	394	0.3
38	Bantu HP	19 May 2019	8.789	38.338	2079	50[b]	28.5	629	7.2	349	0.3
39	Bantu Artesian	19 May 2019	8.786	38.336	2078	350[b]	49.9	1397	8.3	474	<0.1
40	Bantu MS	19 May 2019	8.784	38.337	2080	294	43.2	1082	7.5	405	0.1
	Koka										
14	Gallon China Well	10 May 2019	8.825	38.869	2093	202	26.1	680	7.3	449	4.2
31	HD1[a]	16 May 2019	8.349	38.995	1594	10	24.4	1938	7.4	735	2.3
32	HD2[a]	16 May 2019	8.316	38.969	1614	26	29.1	1031	7.5	562	1.8

[a] Samples taken from static container owing to low flowrate.
[b] Depth estimated from T and SEC measurements in nearby boreholes.
[c] Long surface pipework, significant cooling possible.

high-relief catchment.

3.2. Trace gases

The CFCs (or chlorofluorocarbons) are non-toxic anthropogenic compounds of the halocarbon family. Traces of these have been accumulating in the atmosphere since the 1930s due to release during industrial processes, with a known record of atmospheric mixing ratios. The three main compounds are CFC-11 (CCl_3F), CFC-12 (CCl_2F_2) and CFC-113 ($C_2Cl_3F_3$), with atmospheric lifetimes of 45, 110 and 85 years respectively according to the World Meteorological Organisation (WMO). They have been added to the atmosphere at a known rate, though are now in decline because of a worldwide production ban due to their ozone-depleting properties. Under favourable conditions (no contamination or reduction) they can give quantitative groundwater 'piston flow' ages up to 70 years, although because each reached its atmospheric peak in the 1990s there can be ambiguities for younger water ages (Darling et al., 2012). Under less favourable conditions they still record the presence of 'modern' (≤70 yr old) groundwater, even if the proportion is not calculable.

SF_6 (or sulphur hexafluoride) is another non-toxic anthropogenic compound that has been building up in the atmosphere since the 1970s with an estimated atmospheric lifetime >1000 years, and also the consequence of industrial activities. It can act as a check on the interpretation of the CFCs but is limited to maximum piston flow ages of ~50 years (Darling et al., 2012).

The solubilities of both the CFCs and SF_6 are temperature-related, so this needs to be factored into any interpretation of results. Adjustments ideally also need to be made to correct for likely elevations and temperature of recharge, though in practice these tend to largely cancel out. In addition, SF_6 as a low-solubility gas may need correction for 'excess air' (EA), a condition deriving from aquifer water-table fluctuations. All these aspects are covered in Darling et al. (2012).

3.3. Carbon isotopes

The radiocarbon dating of groundwater, or more accurately its dissolved inorganic carbon (DIC) content, uses the equation:

$$t = -8267 \times \ln\left(a^{14}C_{DIC} / (q \times a^{14}C_{soil})\right) \quad (1)$$

where t = time in yr (in 'radiocarbon years', i.e. uncalibrated:

Table 2
Isotopic and trace-gas analyses of groundwater samples collected in the Upper Awash basin. Also included are estimated recharge elevations (RE) inferred from Fig. 4a, and corresponding recharge temperatures (RT) based on the Koka–Sendafa temperature lapse rate, and trace-gas mixing ratios based on conversion from measured concentrations, with SF_6 additionally corrected for excess air.

Site	$\delta^{18}O$ ‰ VSMOW	$\delta^{2}H$ ‰ VSMOW	$\delta^{13}C$-DIC ‰ VPDB	^{14}C-DIC pmc	±	CFC-12 pmol/L	CFC-11 pmol/L	CFC-113 pmol/L	SF_6 unc fmol/L	**RE m asl**	**RT °C**	**CFC-12 pptv**	**CFC-11 pptv**	**CFC-113 pptv**	**SF_6 pptv**
Akaki															
1	−2.91	−11.6	−9.33	25.9	0.8	0.17	0.23	0.05	0.17	2460	15.4	52.2	19.4	13.4	0.44
2	−2.53	−6.7	–	–	–	0.38	0.44	0.11	1.18	2400	15.9	121	37.7	31.8	2.95
3	−4.20	−17.9	–	–	–	1.23	3.46	0.13	1.75	2310	16.8	459	348	45.3	4.91
4	−4.20	−17.3	−6.64	30.0	0.8	0.06	0.04	0.04	0.07	2310	16.8	18.9	3.4	12.2	0.17
5	−4.88	−22.4	−2.64	1.64	1.0	–	–	–	–	2900	11.2	–	–	–	–
6	−2.99	−10.0	−9.70	–	0.8	0.15	0.48	0.04	0.14	2470	15.3	46.1	39.9	10.4	0.35
7	−2.85	−6.9	–	–	–	0.49	2.29	0.17	0.07	2470	15.3	152	190	45.7	0.18
8	−1.67	−1.3	−6.55	85.6	0.4	0.07	0.34	0.04	0.03	2070	19.0	26.1	32.1	13.3	0.07
9	−1.82	−1.6	−7.18	88.1	0.4	0.24	1.11	0.13	0.14	2060	19.1	85.0	106	41.1	0.34
10	−4.56	−21.8	−8.05	54.4	0.6	0.06	0.15	0.04	4.77	2610	14.0	18.0	11.9	10.3	11.8
11	−2.43	−10.1	−7.58	76.9	0.4	0.12	0.37	0.04	0.08	2060	19.1	41.3	35.3	14.4	0.20
12	−3.95	−18.7	−9.11	29.4	0.8	<0.01	0.16	0.04	0.07	2100	18.8	<1.7	15.2	13.3	0.17
13	−2.11	−5.9	−7.08	81.9	0.4	–	–	–	–	2070	19.0	–	–	–	–
17	−1.73	−0.2	–	–	–	0.61	1.20	0.14	0.13	2290	17.0	201	108	42.3	0.33
18	−4.95	−20.5	−9.44	8.56	1.0	–	–	–	–	2940	10.9	–	–	–	–
Mojo															
15	−1.12	1.1	–	–	–	0.64	1.03	0.11	0.06	1900	20.6	237	105	39.5	0.13
16	−3.36	−13.2	−6.83	49.4	0.6	0.06	0.08	0.04	0.05	1890	20.7	23.8	7.7	14.5	0.13
19	−3.72	−17.7	−8.89	60.2	0.5	0.11	0.22	0.04	0.19	1900	20.6	43.1	23.2	12.1	0.46
20	0.89	8.5	–	–	–	0.44	0.81	0.13	0.02	1890	20.7	162	82.0	40.4	0.05
21	−1.88	−5.2	−8.89	79.6	0.4	0.07	0.02	0.02	0.14	1890	20.7	27.7	2.0	5.4	0.34
22	−4.48	−24.3	−7.89	55.7	0.6	0.05	0.13	0.03	0.14	2540	14.6	14.1	10.1	7.3	0.32
23	−4.89	−26.4	–	–	–	0.12	0.22	0.04	0.28	2880	11.4	35.5	16.6	9.3	0.69
24	−4.95	−26.1	−7.53	58.9	0.5	0.10	0.12	0.03	0.19	2930	11.0	28.8	9.1	7.3	0.46
25	−4.20	−22.6	–	–	–	1.00	2.89	0.16	1.35	2310	16.8	340	265	50.4	3.45
26	−1.70	−7.2	−6.21	48.5	0.6	–	–	–	–	1600	23.5	–	–	–	–
27	−5.03	−25.2	−7.58	58.5	0.5	0.02	0.34	0.28	<0.01	3000	10.3	4.5	23.8	64.3	–
28	−3.22	−17.3	−4.13	24.8	0.8	–	–	–	–	1590	23.6	–	–	–	–
29	−3.82	−19.8	−6.76	61.1	0.5	0.32	0.35	0.06	0.40	1990	19.8	117	35.1	21.6	0.99
30	−2.39	−12.1	−9.15	83.9	0.4	0.23	0.30	0.06	0.16	1590	23.6	91.0	33.5	23.1	0.34
Melka Kunture															
33	−4.31	−21.2	−6.56	22.0	0.9					2400	15.9	–	–	–	–
34	−4.06	−18.7	−7.05	43.4	0.7	0.05	0.07	0.01	0.03	2190	17.9	18.3	6.9	3.9	0.06
35	−4.46	−23.5	−4.77	57.6	0.5	0.04	0.07	0.02	0.02	2530	14.7	11.4	6.1	6.4	0.06
36	−4.36	−23.5	–	–	–	–	–	–	–	2440	15.6	–	–	–	–
37	−4.11	−18.8	−5.86	45.3	0.5	0.10	0.13	0.04	0.09	2230	17.5	34.9	12.6	12.9	0.22
38	−4.26	−20.3	−6.76	56.4	0.5	0.05	0.33	0.08	0.03	2360	16.3	14.7	29.0	24.2	0.08
39	−5.56	−28.5	–	–	–	1.48	6.51	0.24	3.02	3440	6.2	345	383	44.9	6.59
40	−5.01	−25.1	−5.02	13.5	0.9	0.06	0.05	0.02	0.04	2980	10.5	16.7	3.6	4.1	0.10
Koka															
14	−2.31	−4.8	−13.35	86.0	0.4	0.01	0.25	0.04	0.01	2100	18.8	3.4	23.5	14.4	0.03
31	−1.39	−1.6	–	–	–	–	–	–	–	1590	23.6	–	–	–	–
32	−1.14	0.4	–	–	–	–	–	–	–	1610	23.4	–	–	–	–

Cartwright et al., 2020).

$a^{14}C_{DIC}$ = ^{14}C activity of the sample water in pmc (percent modern carbon).

$a^{14}C_{soil}$ = ^{14}C activity of soil inorganic carbon in pmc.

q = dilution factor.

The dilution factor is intended to correct for any inputs of carbon from old ^{14}C-dead sources. In the UAB there could be several. There is evidence for mantle CO_2 reaching the Akaki catchment in the thermal waters associated with the previously mentioned Filwoha Graben (Demlie et al., 2007) and the possibility of mineralised carbon from organic-rich palaeolake sediments preserved beneath basalt flows (e.g. Benvenuti et al., 2002) Methane, on the other hand, is unlikely to be a significant contributor as its concentration in ground gases in the rift valley area is low (Darling, 1998).

The approach here is based on using $\delta^{13}C$ to calculate the notional q-value for each sample (Pearson and Hanshaw, 1970; Clark and Fritz, 2013). Values are then fed into eq. (1) to calculate the ^{14}C age of each site (a soil zone activity of 100 pmc is assumed).

$$q = (\delta^{13}C_{DIC} - \delta^{13}C_{carb})/ (\delta^{13}C_{soil} - \delta^{13}C_{carb}) \quad (2).$$

where $\delta^{13}C_{DIC}$ = ^{13}C measured in the water (‰) $\delta^{13}C_{carb}$ = ^{13}C of 'dead' carbon from carbonate minerals in the aquifer rock (‰) $\delta^{13}C_{soil}$ = ^{13}C of carbon in soil-zone CO_2 (‰)

For $\delta^{13}C_{carb}$, a value of 0‰ has been used as being typical of the MER environment (Darling et al., 1996; Bretzler et al. 2011). For $\delta^{13}C_{soil}$, it is assumed that in a typically mixed C3/C4 highland vegetational environment (Eshetu and Högberg, 2000) a mean value of –16‰ is appropriate (Bretzler et al., 2011). An individual value of q is thereby calculated for each site.

Even allowing for this correction, it should be noted that (i) uncertainties over past soil-zone radiocarbon activities can lead to underestimates of age (Cartwright et al., 2020), while (ii) ^{14}C-based groundwater model ages <~1 kyr are generally regarded as invalid due to the combination of uncertainties (Han and Wassenaar, 2021).

4. Sampling and analysis

4.1. Sampling

Borehole locations were selected to represent the range in

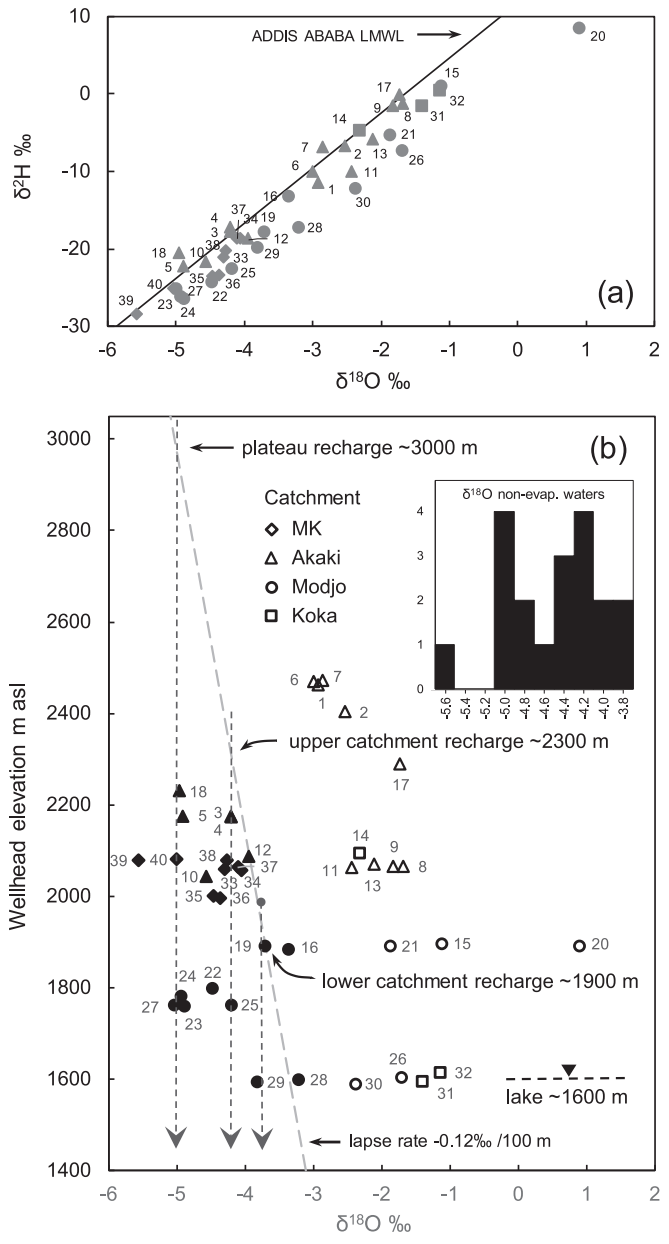

Fig. 2. (a) Plot of $\delta^{18}O$ vs $\delta^{2}H$ for all samples collected in the study shown in relation to the local meteoric water line (LMWL) for Addis Ababa (data from https://nucleus.iaea.org/wiser/index.aspx); (b) Plots of wellhead elevation vs $\delta^{18}O$ value for all sampled sites in relation to the inferred local lapse rate. Samples plotting on or to the left of the line are assumed to derive from the same or higher elevation (vertical projection), while samples plotting ≥ 1‰ horizontally to the right of the line are assumed to contain at least some evaporated water. (Samples are sub-divided according to catchment (symbol shape) and whether they contain a surface-water component inferred from their $\delta^{18}O$—elevation relationship (open symbols).

topographic elevation across the catchment from 2470 m on the Upper Plateau to 1590 m in the Rift Valley (Fig. 1; Table 1). At similar surface elevations, where possible, several boreholes penetrating to varying depths were selected to allow multi-depth sampling to investigate vertical connectivity of the aquifer. Overall borehole depths ranged from 10 to 780 m (Table 1). In a limited number of cases (seven), there was no information about borehole depth so this was inferred by comparison with neighbouring boreholes on the basis of temperature, SEC (specific electrical conductivity) and stable isotope evidence. There is limited information concerning borehole completion and inflows: boreholes are typically screened across all water bearing horizons to maximise potential yield, in which case water samples will represent a mixed signal.

All boreholes were in supply at the time of sampling, but it was confirmed that the field parameters of temperature, pH, SEC and DO (dissolved O_2) had stabilised prior to sample collection.

Samples for stable isotopes and chemistry were collected at all sites in HDPE bottles usually directly from a flowing tube, though in few cases (Table 1) rapid drawdowns necessitated collection of a bulk sample which was then subdivided. Samples for ^{14}C analysis were collected from a subset of sites in 1-litre HDPE bottles. Samples for trace gas measurement were collected from flowing tubing in submerged glass bottles. Trace gas samples were not collected from boreholes where it was too hot (>45°C) to safely seal the bottle and/or where the pump was surging and drawing in air. Nevertheless, 31 of the 40 sites were considered suitable for trace gas sampling.

4.2. Analysis

Stable isotopes were measured by dual-inlet IRMS (Isotope Ratio Mass Spectrometry) at BGS-Keyworth. Trace gases were analysed by GC-ECD (Gas Chromatography with Electron Capture Detector) at BGS-Wallingford. Radiocarbon activities were determined by AMS (Accelerator Mass Spectrometry) following preparation at RCD Lockinge Ltd, Wantage, UK. Inorganic hydrochemistry was analysed by ICP-MS (Inductively Coupled Plasma Mass Spectrometry) and ion chromatography at BGS-Keyworth.

Stable isotope measurement precisions were within ± 0.1‰ ($\delta^{18}O$), ±1‰ ($\delta^{2}H$) and ± 0.2‰ ($\delta^{13}C$-DIC). CFC detection limits were 0.01 (CFC-11) and 0.03 pmol/L (CFC-12 and CFC–113), while the SF_6 detection limit was 0.01 fmol/L. Precisions for ^{14}C averaged ± 0.6 pmc (percent modern carbon, i.e. unnormalized) with individual results being reported in Table 2.

5. Results and interpretation

5.1. General characteristics

Sample water temperatures covered a range of almost 50°C, from 21.2°C on the plateau to 68.1°C on the Rift floor, though were poorly correlated with both wellhead elevation ($r^2 = 0.04$) or borehole depth ($r^2 = 0.08$). SEC values ranged from a comparatively dilute 295 µS/cm on the plateau to a highly-mineralised 2600 µS/cm on the rift floor, and showed a moderate correlation with water temperature ($r^2 = 0.54$). Values of pH were generally in the ranges 7–8 units, but were poorly related to alkalinity ($r^2 = 0.10$). However, alkalinity was strongly correlated with SEC ($r^2 = 0.86$) as would be expected in a region where bicarbonate is the dominant cation. Around one-third of the waters were moderately-to-well-oxygenated (>2 mg/L), but more than half the remainder were significantly below 1 mg/L and therefore tending towards anoxia.

5.2. Sources of recharge

Stable O and H isotopes (Table 2) are often used in groundwater studies as a basic screening tool for sources of recharge (Clark and Fritz, 1997). A delta-plot (Fig. 2a) reveals a similar range of samples as previous studies focusing on the UAB (Demlie et al., 2007, 2008; Yitbarek et al., 2012), with a comparatively wide spread of datapoints due to a combination of the basin relief and evaporative enrichment effects, the latter being very clear for Site 20 but less so for most other sites. Therefore some additional assistance with sifting the data is necessary.

To do this, we have taken $\delta^{18}O$ (more sensitive to evaporation effects than $\delta^{2}H$) and plotted it relative to wellhead elevation for each site (Fig. 2b). The Blue Nile catchment gradient of –0.12‰/100 m (Kebede and Travi, 2012; Tekleab et al., 2014) is assumed to also apply in the neighbouring UAB. The intercept (controlling where the lapse line

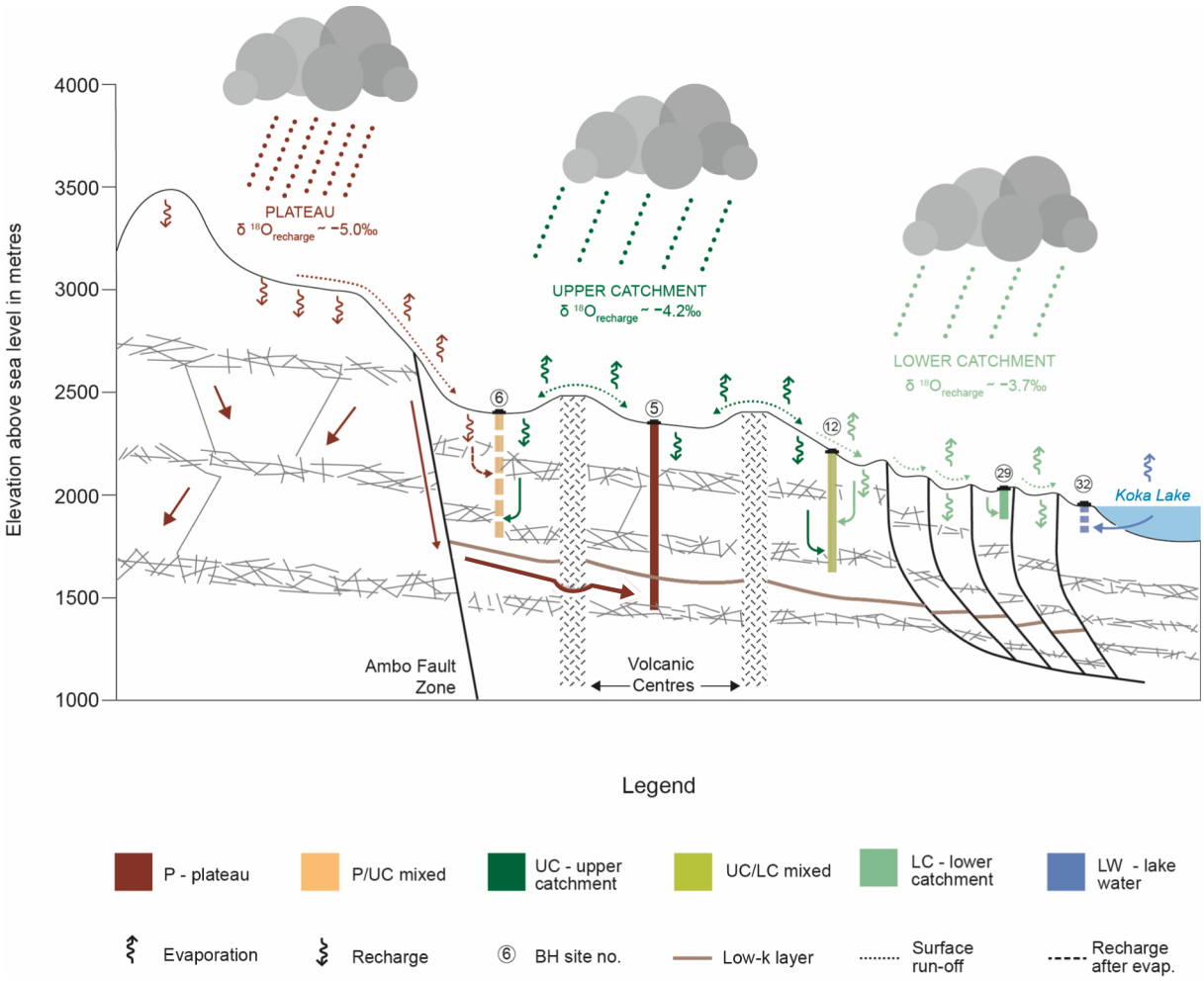

Fig. 3. Schematic conception of $\delta^{18}O$ systematics in the Akaki catchment of the Upper Awash basin, superimposed on a cross-section adapted from Demlie et al. (2007). Direct infiltration ($\delta^{18}O_{recharge}$) is assumed to be isotopically selected but basically unfractionated, while surface runoff is fractionated to varying extents by evaporation before (re)infiltration. Five specimen borehole sites are used to show how different $\delta^{18}O$ values could arise. The Ambo fault zone is assumed to direct most plateau recharge to a deep flow system. Volcanic feeders are not considered to form major barriers to lateral flow. The position of selected borehole sites, and their inferred inflow horizons, are indicative rather than exact. From the highest elevation downwards: P – plateau; UC – upper catchment; LC – lower catchment; LW – lakewater.

crosses the x-axis in Fig. 2b) can be inferred from a case where recharge is likely to be local in elevation. Here this is represented by the most isotopically depleted sample from the Bishoftu maar area (location: Fig. 1). Site 19 (Shimbara BH11) abstracts from an aquifer considered by Kebede et al (2001) to result from low-residence recharge into the surrounding porous basalt. Unlike some adjacent sites where there is mixing with maar lakewaters (15, 20, 21), site 19 shows little or no evidence of evaporative enrichment (Fig. 2a).

The $\delta^{18}O$ data from all sites plot on either side of the lapse line (Fig. 2b). Those to the left are assumed to represent water recharged at an elevation defined by the point where a vertical projection meets the lapse line. Thus, for example, a $\delta^{18}O$ value of –5‰ would indicate recharge at 2900–3000 m asl, which is the average height of the plateau around the basin. A histogram (inset to Fig. 2b) suggests that most of the waters fall into one of two clusters: around –5.0 and –4.2‰, the latter coinciding with what can be termed 'upper catchment' averaging around 2300 m asl. Less clearly, there is a suggestion of a third level of recharge at a 'lower catchment' value of ~ –3.7‰ and an elevation of 1900 m asl. Groupings by elevation are not restricted to a single catchment, so are presumed to apply across the basin (Fig. 2b).

In contrast, we hypothesise that samples plotting to the right of the lapse line have to a greater or lesser extent been affected by evaporation, which has the effect of raising $\delta^{18}O$ (and $\delta^{2}H$, Fig. 2a) to values too isotopically enriched to have resulted from rainfall inputs alone within the UAB. The evaporated component of the waters is assumed to be derived from surface exposure, in the form of a watercourse, ponding, lake or irrigation return at some point in the sample's history. This in turn would most likely affect its hydrogeochemical properties and therefore will require further consideration below (5.4). Samples believed to contain a surface-water component are shown as empty symbols in Fig. 2b, and in subsequent figures where relevant.

For simplicity, only wellhead elevations are used in Fig. 2b to demonstrate general relationships. However, borehole depths need to be factored into any attempts to arrive at a hydrogeological interpretation. The approach taken here assumes that the isotopic value of water from individual boreholes is the product of the contributing recharge elevation(s) plus surface water contribution, if any. Where waters appreciably differ from the three defined recharge types inferred from Fig. 2b (i.e. plateau, upper catchment and lower catchment), they are assumed to be mixtures, with inputs to the borehole at a level inversely proportional to recharge elevation (i.e. plateau recharge will enter the bore at a lower level and higher head than upper catchment recharge). Boreholes with a surface water component are indicated as broken lines; the surface component is assumed to enter the bore at a higher level than the groundwater.

A schematic of how this might operate for selected sites is depicted in

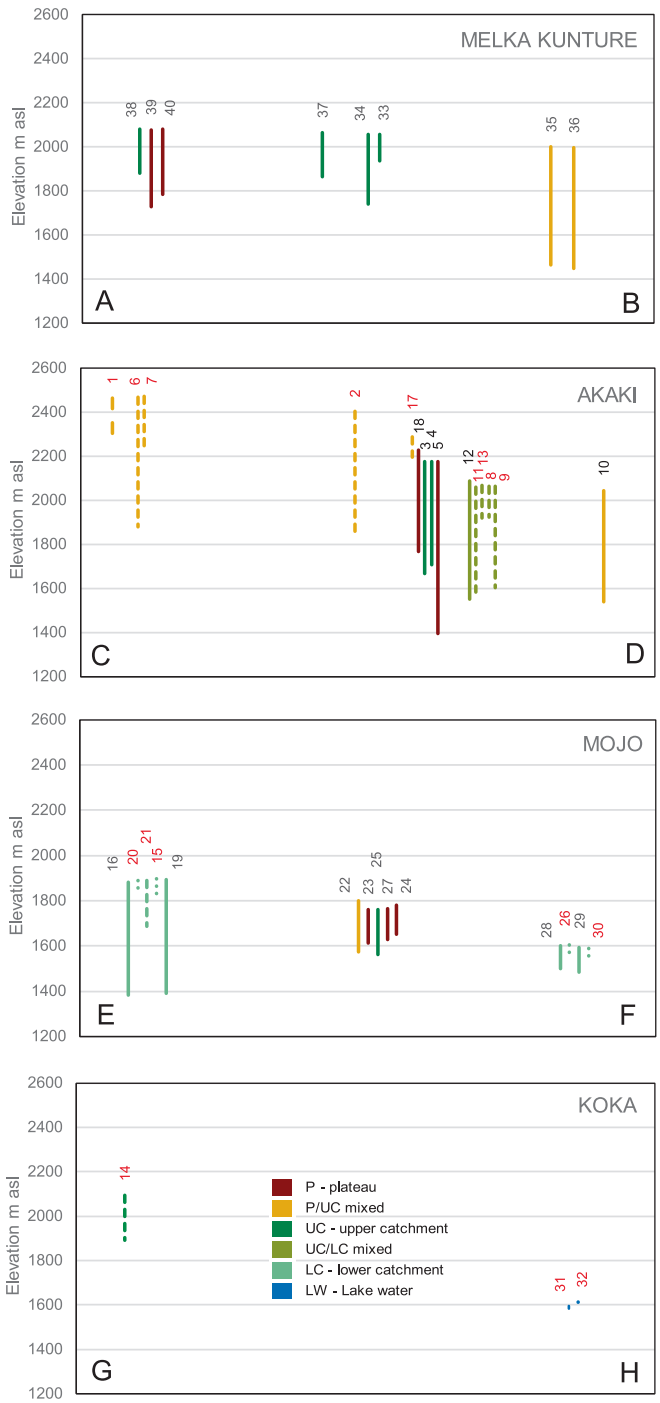

Fig. 4. Schematic sections showing borehole depths vs elevation along transects in the various Upper Awash catchments shown on Fig. 3. Borehole colour shows probable recharge source(s) based on $\delta^{18}O$ (see legend). Broken lines and red site numbers indicate sites with an inferred surface water component. (For interpretation of the references to colour in this figure legend, the reader is referred to the web version of this article.)

Fig. 3, which uses elevation-based colour coding taken from Fig. 1. More precisely, Fig. 4 shows all boreholes from the study plotted by catchment along the transect lines shown in Fig. 1 (although Fig. 3 is based on the Akaki, it is assumed that all the catchments operate in a similar way isotopically). All boreholes are plotted to the same vertical scale but horizontal separations vary somewhat between catchments due to the variation in section line length (Fig. 1).

The four catchments vary considerably in apparent degree of complexity (Fig. 4). The MK catchment (Fig. 1, section A–B) presents a relatively simple picture of recharge from the plateau, or from the upper catchment, or in two cases (Sites 35 and 36) a mixture of the two. There is no isotopic evidence for surface water entering any part of the system.

The Akaki catchment (Figs. 1 and 4, section C-D) is the most heavily-developed in the basin, accommodating Addis Ababa and therefore likely to be most impacted by abstraction. At the top end of the catchment, boreholes near watercourses in the Big Akaki river system (sites 1, 2, 6, 7) are abstracting a mixture of plateau and upper catchment water: the plateau component is assumed to be contributing the evaporated signal to the mixture (streams in the area show the required isotopic enrichment: Yitbarek et al., 2012; Tadesse et al., 2023). Similarly high in the Little Akaki valley, Site 17 is also affected by additions of plateau stream water, though the neighbouring much deeper borehole 18 taps unmodified plateau water. Further down catchment, the Heineken Brewery boreholes show either an upper catchment source (sites 3 and 4), or a plateau source in the deepest (5). By contrast, sites 8, 9, 11, 12 and 13 are all producing a mixed upper-lower catchment water, usually with a surface component assumed to originate from the upper catchment. This grouping includes the important Akaki Wellfield (Birhanu et al., 2021). Lastly, Site 10 is situated below the disused Aba Samuel reservoir but unlike the previous group is a mixture of plateau and upper-catchment recharge with no evaporated component, so is assumed not to be drawing in any surface water. Although quite far down-catchment, higher ground lies nearby to the west which could be contributing isotopically-depleted water.

In the Mojo catchment (Figs. 1 and 4, section E–F), all sampled boreholes are situated on lower ground with wellheads no higher than 'lower-catchment' elevation (1900 m), which seems to be the source of water around Bishoftu. However, at sites 15, 20 and 21 there is an evaporated component, probably derived from mixing with surface waters exposed in the water-table lakes formed by several large maar craters (Kebede et al., 2001). The group of boreholes around Mojo town on the other hand appear to be sourced solely from the plateau (sites 23, 24, 27), the upper catchment (25), or a mixture (22).

The Koka catchment is represented by only three boreholes (Figs. 1 and 4, section G–H). Site 14 has a mixed upper-lower catchment origin, with a surface water component presumably sourced from the upper catchment. Despite being on the other side of the topographic divide from the Akaki Wellfield, Site 14 appears to share the same mixed water sources, implying that hydrogeologically it is part of the Akaki catchment. Sites 31 and 32 appear from Fig. 2 to have a lower catchment origin, but their proximity to Lake Koka would imply some evaporated lake water is also being drawn in (though evaporation from minor local ponding in the vicinity or directly from shallow groundwater could also be occurring).

5.3. *Age of waters*

When discussing the 'age' of waters, it needs to be recalled that the values based on data from a particular analytical process are simply tracer ages, which usually depend on one or more assumptions such as no mixing or dispersion, which may or may not be valid (McCallum et al., 2015). They are therefore not necessarily close to describing the real derivation or residence time of the sampled water. However, in the absence of more detailed hydrogeological information, they should at least have some comparative value.

The trace gas concentrations reported in Table 2 are the result of dissolution over a range of temperature conditions according to the $\delta^{18}O$ data, i.e. plateau to rift valley. To make the analyses directly comparable, they have been converted from concentrations to atmospheric mixing ratios by correcting for recharge elevation and temperature. In the case of SF_6, an additional correction for excess air (Darling et al., 2012) has been applied based on a value of 5 cm^3STP/L the average calculated from noble gas analyses from a subset of seven sites, not reported here, using the method of Aeschbach-Hertig et al. (2000).

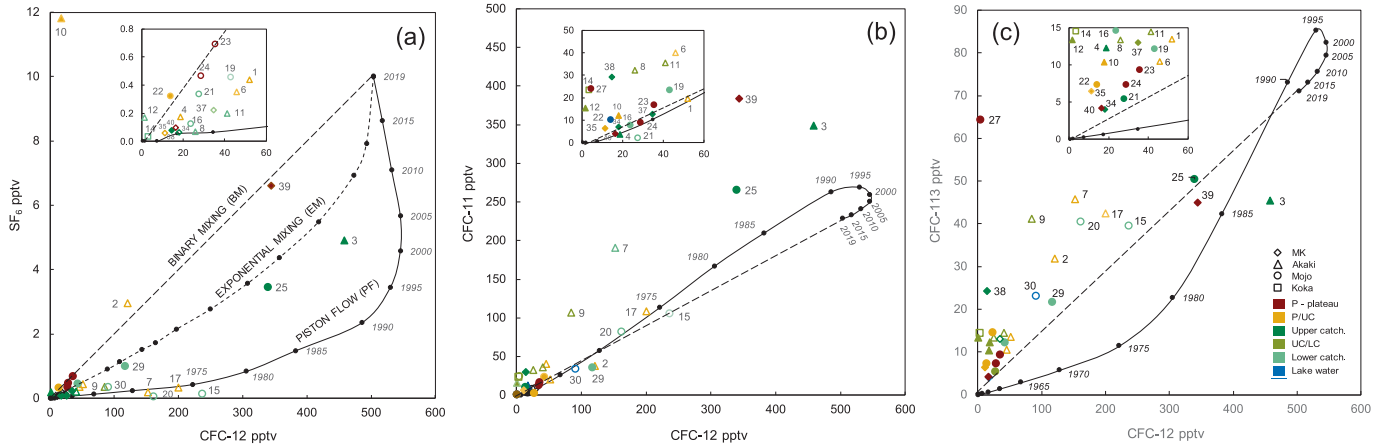

Fig. 5. Cross-plots of trace-gas mixing ratios in pptv (parts per thousand by volume) from Table 4, (a) SF_6 vs CFC-12, (b) CFC-11 vs CFC-12, (c) CFC-113 vs CFC-12, by catchment and probable elevation of origin based on Figs. 2 and 4. Also shown are the atmospheric inputs from USGS (2022) and notional LPM curves for binary mixing (BM), exponential mixing (EM) and piston flow (PF). (EM line not shown in (b) and (c) for clarity.) Insets show site numbering close to the plot origins. Symbols (see legend in 6c) show catchment (shape) and probable recharge source(s) (colour). Empty symbols indicate samples with an inferred surface water component.

Table 3
Results of δ^{13}C-based correction of radiocarbon age for waters from selected sites in the Upper Awash basin. The'mod' values indicate the water is too modern to yield a ^{14}C age based on the assumptions set out in Section 3.3.

Site No.	Temp	HCO_3	δ^{13}C-DIC	^{14}C-DIC	q-value	Age corr.
	°C	mg/L	‰ VPDB	pmc		kyr
Akaki						
1	25.6	234	−9.3	25.9	0.58	6.7
4	32.9	390	−6.6	30.0	0.42	2.7
5	61.5	552	−2.6	1.6	0.17	19.1
6	28.1	244	−9.7	26.2	0.61	6.9
8	24.9	280	−6.5	85.6	0.41	mod
9	24.4	282	−7.2	88.1	0.45	mod
10	36.0	289	−8.0	54.4	0.50	mod
11	25.3	335	−7.6	76.9	0.47	mod
12	39.3	293	−9.1	29.4	0.57	5.5
13	24.5	290	−7.1	81.9	0.44	mod
18	66.3	199	−9.4	8.6	0.59	16.0
Mojo						
16	32.7	385	−6.8	49.4	0.43	mod
19	29.9	302	−8.9	60.2	0.56	mod
21	26.2	360	−8.9	79.6	0.56	mod
22	33.9	400	−7.9	55.7	0.49	mod
24	28.8	324	−7.5	58.9	0.47	mod
26	37.8	622	−6.2	48.5	0.39	mod
27	28.6	317	−7.6	58.5	0.47	mod
28	68.1	966	−4.1	24.8	0.26	0.3
29	43.4	756	−6.8	61.1	0.42	mod
30	33.5	1056	−9.2	83.9	0.57	mod
Melka Kunture						
33	24.1	256	−6.6	22.0	0.41	5.1
34	26.4	258	−7.0	43.4	0.44	0.1
35	26.9	317	−4.8	57.6	0.30	mod
37	22.4	394	−5.9	45.3	0.37	mod
38	28.5	349	−6.8	56.4	0.42	mod
40	43.2	405	−5.0	13.5	0.31	7.0
Koka						
14	26.1	449	−13.4	86.0	0.83	mod

Cross-plots of the trace gases SF_6 and CFCs (Fig. 5a-c) with superimposed LPM curves (Lumped Parameter Model – Zuber and Małoszewski, 2001) show the predominance of water with an apparent age > 50 yr and the absence of severe trace-gas contamination. (CFCs can undergo reduction under low-DO conditions but SF_6 is not affected, so the generally-matching low SF_6 values suggest this has not been an issue for most sites.) In Fig. 5a, samples where separable generally divide into piston flow (PF, sites 7, 15, 17, 20, 30) of 50 + years, exponentially mixed (EM, sites 3 and 25) 20–25 years, and binary mixed (BM, sites 2 and 39) at about 25 and 70% recent water respectively. One site (10) near the Aba Samuel reservoir dam, yields the only identified example of SF_6 contamination in the UAB, possibly due to contamination originating from high-voltage equipment in the former hydro-electric plant (e.g. Fulda and Kinzelbach, 2000).

Fig. 5b and 5c show varying amounts of CFC contamination. CFC-113 is the most water-soluble of the CFCs and would be expected to dominate pollution; Fig. 5c suggests this is the case in the UAB, especially in the case of site 27 in the Bishoftu area. Otherwise, the sites showing significant CFC-113 contamination (2, 7, 9, 17, 20, 38) all have stable isotope evidence for a surface water component and are mostly from the Akaki catchment. The highest-concentration site for CFC-11 (site 39, Fig. 5b), however, has a normal CFC-113 composition, agreeing with the CFC-12 vs SF_6 plot (Fig. 5a) that this source in the MK catchment abstracts mostly recent water. This may seem surprising for a water considered to derive from the plateau, but there is no *a priori* reason why such groundwaters should not have a recent component that is not derived from surface water.

While the conclusion from the trace gases is that many of the waters measured had a <10% recent component, this does not reveal the age range of the majority 'old' water. To investigate this, ^{14}C-DIC was measured on selected samples (Table 2). Values varied from 1.6 to 88 pmc, a large apparent age range. Based on the δ^{13}C age correction (3.3 above), only a quarter of the sites yield an age (Table 3), the remainder calculating out as 'modern', i.e. a few hundred years at most. Values of the dilution factor q vary from 0.83 down to 0.17 (Table 3). The lower the q-value, the greater the amount of inferred dead carbon dilution and therefore uncertainty over the tracer age. The fact that some q-values appear to be strongly affected by temperature (e.g. sites 5 and 28, Fig. 6a) is a sign that at least some of the 'corrected' ages in Table 3 are indicative at best. All sites inferred from δ^{18}O data to yield unmodified groundwater have ^{14}C activities <60 pmc, while those considered to contain an evaporated component are usually >75 pmc (Fig. 6b), implying that recent surface water is contributing, perhaps with a bomb-related ^{14}C activity in excess of 100 pmc (indeed, a value of 112 pmc was recorded for a high-nitrate groundwater on the southern edge of the Koka catchment by Bretzler et al., 2011).

All sites with ^{14}C and CFC-12 data are presented on a cross-plot in Fig. 6c. Sites 1 and 6 in the Akaki catchment show that samples containing evaporated water are not always high in ^{14}C, suggesting that surface water entered before, during recharge or at an early point in the samples' subsurface journey. Conversely, sites 24 and 27 indicate that

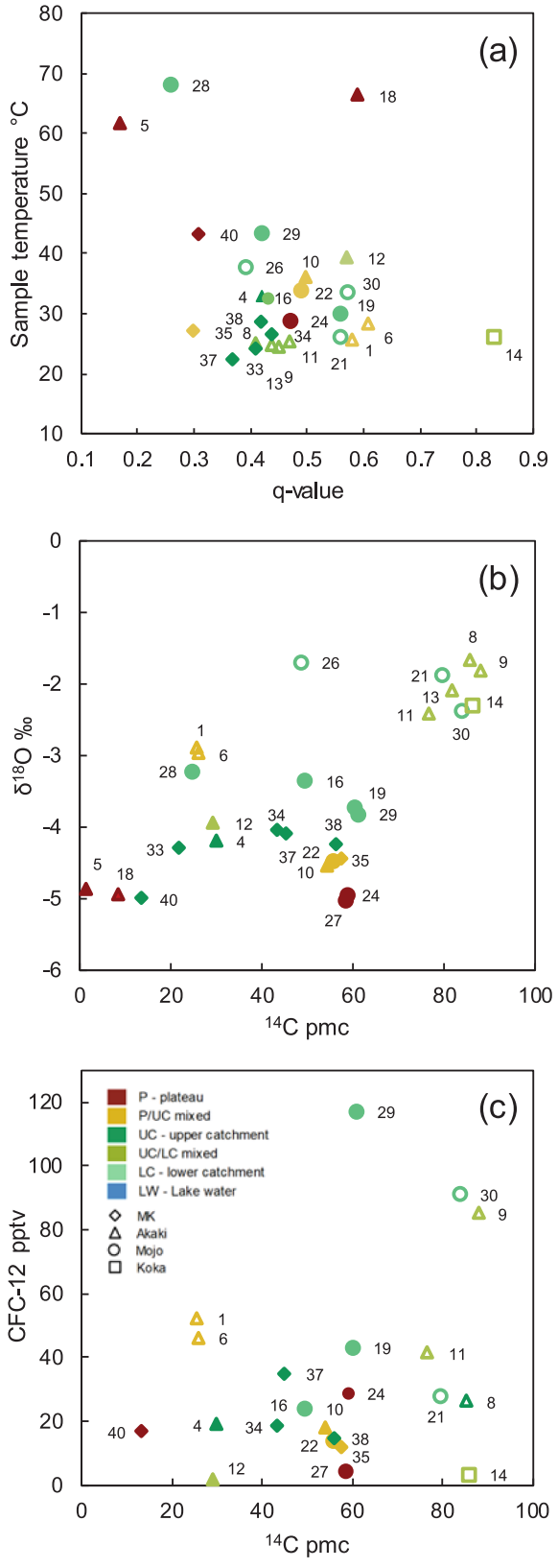

Fig. 6. Residence time information on groundwater samples from the Upper Awash Basin, presented as (a) a plot of temperature vs q-value, (b) as $\delta^{18}O$ vs ^{14}C activity, and (c) CFC-12 mixing ratio vs ^{14}C activity. Symbols (see legend) show catchment (shape) and probable recharge source(s) (colour). Empty symbols indicate samples with an inferred surface water component.

waters deriving from the plateau are not necessarily especially old. Overall, there is little apparent relationship between ^{14}C and CFC-12, suggesting that the 'old' water indicated by the trace gases covers a range of ages (Jasechko et al. 2017).

5.4. Water quality

Table 4 includes major ions plus selected minor and trace species. All waters have HCO_3 as the dominant anion, with only modest contributions from Cl and SO_4 (Fig. 7). In terms of cations there is more variety due to interaction with different lithologies, from higher Mg and Ca in the basalts to Na domination in the more acid volcanics (Yitbarek et al., 2012). However, rather than a simple transition from plateau to rift floor, Fig. 7 indicates variation across the basin and with depth, another indication of geological complexity.

In absolute terms, Fig. 8 shows a cross-plot of SEC vs recharge elevation inferred from $\delta^{18}O$ (5.2 above and Table 2) demonstrating a restricted 'normal' range (435–745 μS/cm) for nearly all samples, with or without a surface water component, except for the plateau-derived samples from sites 5, 39 and 40, the lower catchment samples from sites 28 and 29 and the near-lake sites 26 and 30–32. While the near-lake sites are presumably affected by the drawing-in of high-TDS river or lake water (e.g. Darling et al., 1996), the remainder include most of the thermal (>40°C) waters identified during the study, suggesting that water–rock interaction has been enhanced by the elevated temperature. Significantly though, the high temperatures are poorly correlated with borehole depth ($r^2 = 0.09$ for the whole dataset in Table 1) and therefore indicate the importance of local geological factors in determining upflow of heat. Minor and trace element/ion median concentrations reveal a mixed picture across the four catchments of the UAB (Table 5). The Akaki, Mojo and MK each have eight sites or more, but Koka has only three, one of which (Site 14) is probably hydrogeologically in the Akaki (5.2 above). Waters are divided into those considered to be unmixed, and those believed to have mixed with surface water at some point in their history according to isotopic evidence (5.2 above). While unmixed waters from the MK and Mojo catchments give very similar median values, those from the Akaki are sometimes higher, though notably only in Mn and Fe, implying a geological cause. Waters inferred to be mixed with surface water in the Akaki and Mojo catchments most obviously have much higher median nitrate, presumably connected to the surface water component, as is the dilution of water–rock interaction-derived species like F, Si and Li. Considering that the Akaki is by far the most urbanised catchment of the four, the toxic metal load is little different from Mojo or MK catchments, or between groundwater and mixed water. Certain elements like B are very clearly associated with irrigated floriculture around Koka reservoir, at the foot of both Mojo and Koka catchments, where relatively high concentrations are likely to arise from the lake or river water drawn in by pumping (Yimer and Geberkidan, 2020).

Regarding overall water quality, most waters meet WHO standards (or USEPA where WHO are not available) for As, B, Ba, Cu, Cr, Mn, Ni, NO_3 and Se (Table 4). Cobalt and Zn (unstandardized) are also low, suggesting that widespread urban pollution by metals from industrial processes (e.g. Tarekegn and Weldekidan, 2022) is not yet an issue, at least for the sources considered in this study. Demlie and Wohnlich (2006) recorded some much higher groundwater concentrations locally for Co, Cr, Cu, Ni and Zn from the Akaki catchment, noting that Cr in particular exceeded WHO guidelines, being frequently two orders of magnitude higher than the present results. There are three possible reasons for this: choice of sampling site (possible), major improvement in groundwater quality in the Akaki over the last decade-and-a-half (unlikely), or that the groundwater trace element analytical process has improved over this time period (perhaps most likely). However, some locally high values of Cr were recently observed for a cluster of surface water samples from the central area of Addis Ababa (Aschale et al., 2021) so local leakage to groundwater cannot be ruled out, even if

Table 4
Inorganic hydrochemistry of samples collected in the Upper Awash basin. WHO or USEPA upper limit values (italics) are added for purposes of comparison.

Site	Ca	Mg	Na	K	HCO_3	Cl	SO_4	NO_3	F	Si	Ba	Sr	Mn	Fe_{tot}	Li	B	Cr	Co	Ni	Cu	Zn	As	Se
	mg/L	**mg/L**	**mg/L**	**mg/L**	**mg/L**	**mg/L**	**mg/L**	**mg/L**	**mg/L**	**mg/L**	**µg/L**	**µg/L**	**µg/L**	**µg/L**	**µg/L**	**µg/L**	**µg/L**	**µg/L**	**µg/L**	**µg/L**	**µg/L**	**µg/L**	**µg/L**
	100	*50*	*200*	*20*	*2350*	*250*	*250*	*50*	*1.5*	–	*700*	*7000*	*80*	*300*	*700*	*2400*	*50*	*4*	*70*	*2000*	*3000*	*10*	*40*
Akaki																							
1	30	8.08	47.9	6.98	234	14.7	7.7	0.1	0.85	35.6	52.5	164	105	188	15	<53	<0.07	0.014	0.04	4.97	1.1	<0.04	<0.07
2	37	8.32	57.8	2.61	234	25.4	14.6	19.6	0.70	28.2	21.5	253	102	702	15	<53	0.08	0.423	0.60	4.74	61.9	0.08	<0.07
3	8.0	1.30	152	20.2	374	32.8	13.0	0.1	2.63	47.1	43.8	50	35.4	14.5	73	58	<0.07	0.012	<0.03	2.14	<0.6	4.95	<0.07
4	16	4.12	137	18.8	390	27.3	11.8	0.3	1.90	40.2	29.3	105	15.3	3.5	64	<53	0.08	0.014	0.05	2.31	<0.6	4.24	0.08
5	13	2.86	200	45.1	552	42.0	11.5	0.1	1.46	74.2	51.4	57	16.8	60.2	71	171	<0.07	0.010	<0.03	3.44	<0.6	0.56	<0.07
6	18	4.86	75.6	8.20	244	17.5	6.9	0.1	0.92	35.7	40.4	116	95.4	79.1	16	<53	<0.07	0.008	<0.03	1.10	0.8	0.06	<0.07
7	27	5.77	25.7	3.72	162	3.8	3.1	3.4	0.87	40.8	30.0	156	5.6	4.8	<7	<53	0.16	0.015	0.08	2.04	9.7	0.94	0.41
8	41	24.4	23.0	3.88	280	10.8	6.0	14.1	0.50	31.7	11.0	310	0.9	<0.4	<7	<53	2.6	0.014	0.11	1.29	2.5	0.43	0.32
9	47	26.7	24.7	4.27	282	7.9	7.1	15.7	0.55	32.7	13.5	365	0.8	0.9	7	<53	2.2	0.008	0.19	4.38	33.4	0.51	0.43
10	44	12.6	36.8	8.14	289	3.0	2.8	0.6	1.39	40.1	4.4	226	0.4	<0.4	36	<53	0.12	<0.007	<0.03	2.50	4.7	1.37	0.09
11	60	23.8	37.4	7.09	335	20.1	11.3	20.1	0.60	37.1	13.6	394	1.3	0.5	11	<53	0.38	0.048	0.24	1.75	2.8	0.60	0.40
12	18	5.35	102	7.37	293	22.8	14.5	3.3	3.70	43.4	14.4	113	16.0	35.8	45	<53	<0.07	0.064	0.16	1.28	22.9	4.90	0.17
13[1]	41	24.6	47.3	5.82	290	20.6	9.4	14.1	0.62	26.4	10.1	332	0.4	0.4	<7	<53	2.12	0.012	0.07	2.03	3.4	0.46	0.46
17	65	16.6	24.9	2.08	282	27.7	17.0	6.7	0.65	29.3	35.9	438	0.8	<0.4	<7	<53	<0.07	0.014	0.09	5.35	5.2	0.08	<0.07
18[1]	1.0	0.08	96.4	2.22	199	23.1	4.9	<0.1	4.07	36.3	1.5	5	4.1	45.2	10	94	<0.07	0.051	0.13	0.80	<0.6	5.16	<0.07
Mojo																							
15	73	37.1	28.4	11.9	406	22.2	20.5	23.6	0.68	26.9	46.0	337	1.0	1.0	8	<53	0.71	0.063	0.60	2.02	5.1	2.30	1.12
16	26	25.7	64.1	7.86	385	11.3	7.2	<0.1	0.56	39.5	23.6	195	46.1	11.1	16	<53	<0.07	0.047	0.21	0.97	0.8	2.30	0.09
19	31	15.0	45.0	9.27	302	8.3	6.4	2.8	0.71	41.8	13.7	203	3.8	2.9	10	<53	0.39	<0.007	0.09	1.11	2.7	0.95	0.21
20	62	32.4	18.4	10.8	365	10.0	6.6	16.6	0.79	30.3	44.0	286	0.9	3.9	7	<53	0.64	0.028	0.27	1.98	4.7	1.38	0.34
21	36	34.8	30.4	6.71	360	5.4	3.4	<0.1	0.66	38.6	16.6	227	244	2.8	13	<53	<0.07	0.078	0.17	0.97	2.5	1.61	0.14
22	46	16.6	64.6	16.2	400	12.0	9.7	2.1	1.11	51.5	10.8	220	4.0	<0.4	40	67	0.34	<0.007	<0.03	1.79	6.4	1.63	0.39
23	44	16.8	63.8	15.2	401	12.3	8.4	1.5	1.24	51.6	10.9	211	2.0	3.0	38	67	0.54	<0.007	<0.03	1.53	12.5	4.19	0.36
24	40	9.64	50.6	13.0	324	6.5	5.2	4.1	1.32	52.3	10.1	150	0.6	0.7	32	<53	1.02	<0.007	<0.03	1.02	14.4	1.45	0.33
25	43	18.2	73.0	20.2	418	15.5	9.7	2.9	1.00	54.2	8.5	206	0.5	1.8	40	85	0.13	<0.007	<0.03	0.74	7.7	4.33	0.49
26[1]	10	2.24	330	25.8	622	52.1	52.5	138	9.76	57.6	11.3	139	0.4	4.7	75	390	0.4	1.033	6.97	6.04	1.0	3.73	0.49
27	45	11.4	52.3	12.2	317	6.8	5.3	4.3	1.37	51.7	12.3	144	0.4	2.0	34	54	1.15	0.008	0.13	2.96	21.3	1.63	0.37
28[1]	2.0	0.17	434	21.2	966	55.8	23.3	45.7	18.2	71.1	4.4	17	8.4	11.0	151	598	0.14	0.182	1.97	3.26	9.2	8.63	0.22
29	7.0	1.12	317	24.2	756	38.8	17.4	41.8	12.8	69.6	8.5	58	2.3	4.5	58	392	0.55	0.215	2.00	3.12	2.6	3.97	0.39
30	7.0	1.41	467	27.5	1056	101	16.4	9.8	21.3	57.3	2.8	104	0.4	0.9	100	759	0.31	0.161	0.68	2.56	11.7	6.34	0.37
Melka Kunture																							
33	55	14.1	64.7	5.61	256	48.7	52.0	0.5	0.91	44.5	28.1	398	4.7	1.2	<7	62	0.08	<0.007	0.06	1.21	20.4	0.59	0.57
34	31	9.31	64.4	6.09	258	18.0	21.7	1.4	1.32	41.4	19.5	229	23.5	2.6	13	61	0.09	0.029	0.10	0.45	287	1.66	0.38
35	52	9.43	45.3	9.38	317	6.3	5.9	2.6	1.16	49.8	21.9	257	2.6	1.2	20	<53	0.2	<0.007	0.04	1.00	11.3	0.76	0.18
36	55	11.2	43.3	10.5	328	7.5	6.5	3.4	1.03	49.8	39.5	286	0.9	8.0	19	<53	<0.07	<0.007	<0.03	0.19	82.8	0.83	0.15
37	71	18.6	37.8	7.48	394	4.5	1.3	0.8	0.87	43.2	20.5	425	3.0	0.4	<7	56	2.19	0.009	0.15	0.46	7.8	0.88	<0.07
38	67	8.51	53.4	8.77	349	12.8	9.1	4.7	1.53	45.3	94.7	344	146	52.1	7	69	0.18	0.073	0.04	<0.08	771	1.82	0.50
39	4.0	0.82	246	13.7	474	61.3	74.5	<0.1	1.48	22.0	35.2	26	19.7	56.5	12	305	<0.07	<0.007	<0.03	0.23	4.2	3.51	<0.07
40	4.0	0.44	208	19.5	405	60.8	50.7	<0.1	2.41	69.5	15.4	23	66.5	550	39	305	<0.07	0.017	<0.03	<0.08	50.0	3.91	<0.07
Koka																							
14	53	44.8	29.0	3.25	449	4.3	1.7	5.3	0.27	33.0	10.5	514	1.8	1.6	<7	<53	1.89	0.009	0.29	3.14	5.9	0.17	0.19
31[1]	65	15.3	349	35.6	735	191	38.9	11.5	4.60	40.3	27.9	592	2.7	50.5	69	327	0.78	0.072	0.28	1.64	1.5	1.66	0.71
32[1]	32	3.86	200	12.5	562	53.5	2.9	1.4	7.36	49.8	14.2	63	18.4	6.3	65	215	0.33	0.023	0.34	1.17	3.2	2.13	0.20

[1]Samples taken from static container owing to low flowrate

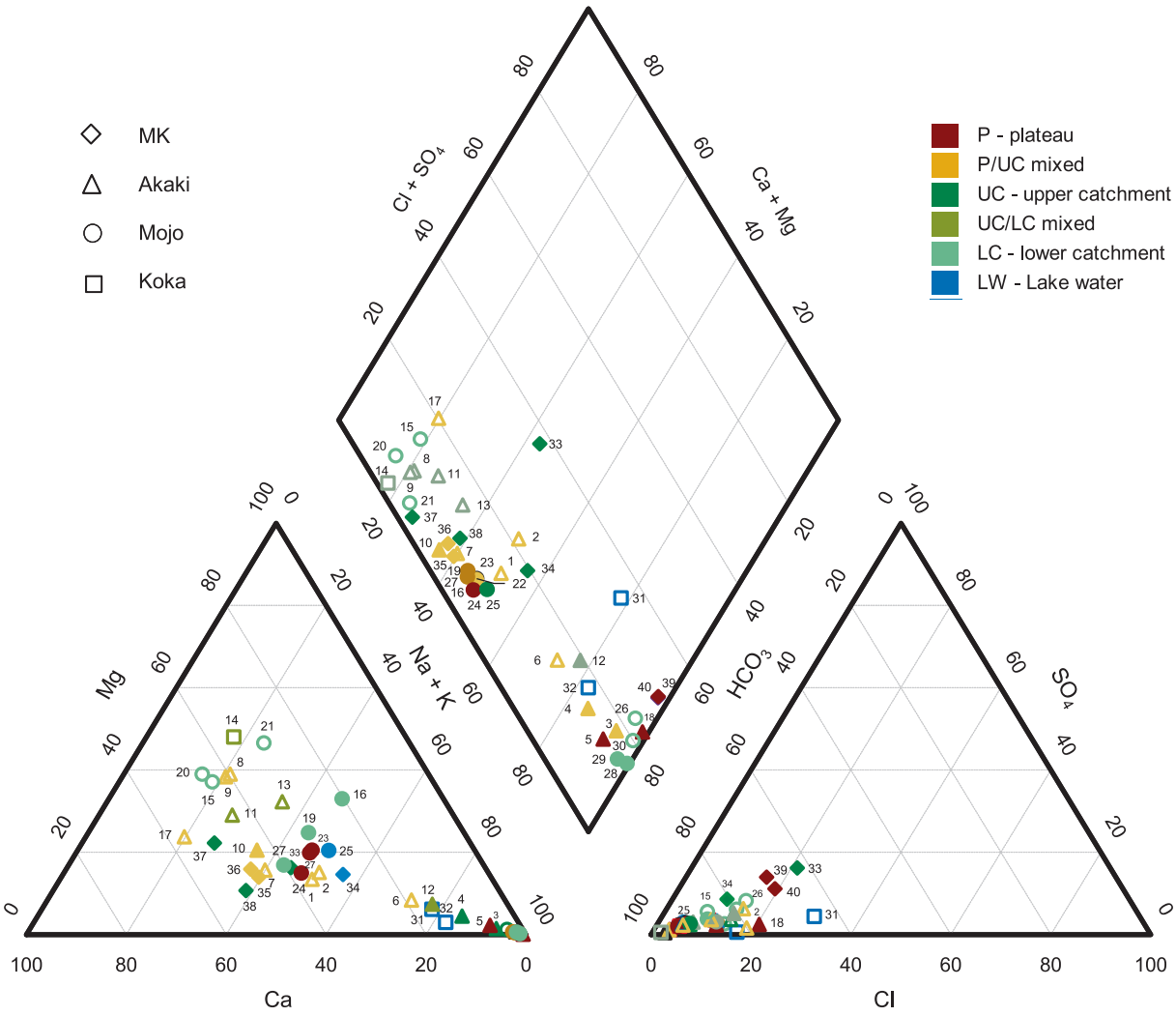

Fig. 7. Piper plot for water samples collected from Upper Awash boreholes. Symbols (see legend) show catchment (shape) and probable recharge source(s) (colour). Empty symbols indicate samples with an inferred surface water component.

the present study did not encounter it.

6. Discussion: groundwater in the upper awash basin

Uncertainties.

The interpretative framework of this study relies to a large extent on the groundwater isotope lapse rate shown in Fig. 2b. To test its validity, reference can be made to its predictions for extreme altitude. The highest elevations reached in the basin catchments are ~ 3500 m, which using the chosen lapse rate would equate to a maximum depletion of –5.7‰ $\delta^{18}O$. The most depleted sample in this study is site 39, with a value of –5.56‰ (Table 2). Other studies within the basin report maximum depletions of the same order, from –5.14 to –5.88‰ (Demlie et al., 2007; Demlie et al., 2008; Kebede et al., 2010; Bretzler et al., 2011; Yitbarek et al., 2012; Tadesse et al., 2023). Therefore, allowing for a typical $\delta^{18}O$ measurement precision of ± 0.1‰, all studies are reporting very similar maximum depletion values for the basin, similar to that theoretically calculated for the highest elevations. Any significant deviation in the lapse-rate intercept would result either in groundwaters being unable to achieve the maximum $\delta^{18}O$ depletions observed to date in the catchments (positive deviation), or that there is little or no plateau-derived recharge in the UAB (negative deviation), both of which appear unlikely.

Some further uncertainty must arise from the general lack of information about borehole construction and inflow horizons. As mentioned in 4.1 above, boreholes are typically screened across all inflows meaning that a certain amount of mixing is to be expected. However, the use of stable isotopes is intended to reveal cases where mixing is likely to be occurring, rather than relying on borehole details.

Origin of recharge.

With the above provisos in mind, Figs. 2b and 4 can be used to estimate the elevation of recharge to sampling points. From the upper catchment downwards this is likely to be local to the individual surface catchment, but at the highest level (plateau) there is some ambiguity.

In the embayment off the rift valley hosting the UAB, the Ambo Fault is the dominant E – W structure, forming the northern boundary to the MK, Akaki and Mojo catchments (Fig. 9). Otherwise, sub-parallel NE – SW step-faulting develops progressively down towards the rift floor (Kebede et al., 2008), reflected by the lineations in the terrain. In the MK catchment, the Ambo fault appears to have little or no effect on the water arriving at the sampled boreholes, all of which abstract from plateau or upper catchment sources, or a mixture of the two. While there is no specific evidence that the plateau component is recharged from the direction of the Ambo Fault, as land around the western and southern periphery of the catchment can also reach the 3000 + m elevations necessary to produce the required isotope depletions of ~ –5‰ $\delta^{18}O$ (Fig. 1), the probable existence of groundwater capture from Nile subcatchments (Azagegn et al., 2015) implies that at least some of this is

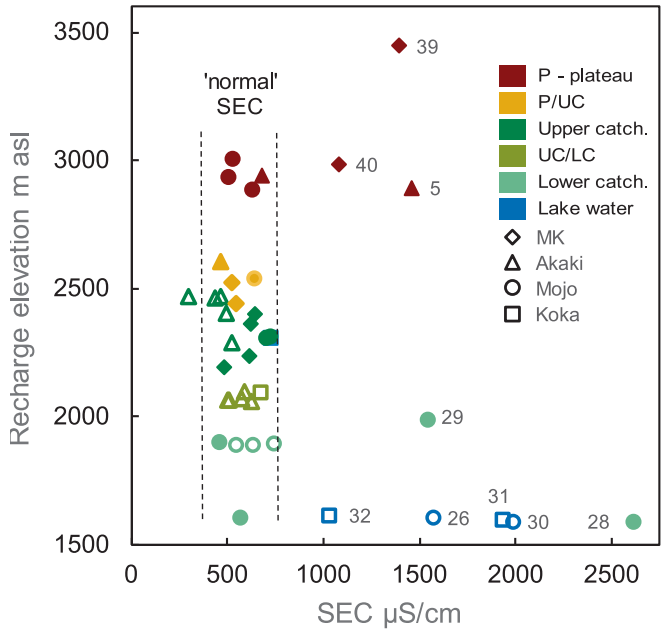

Fig. 8. SEC (specific electrical conductivity) versus recharge elevation inferred from $\delta^{18}O$ value (see Fig. 3). Symbols show catchment (shape) and recharge source(s) (colour). Empty symbols indicate samples with an inferred surface water component.

crossing the fault into the MK system. In the Akaki catchment however, while there is evidence of NE–SW trending structures beginning to play a role (e.g. the Filwoha Graben, which allows the invasion of deep thermal fluids beneath central Addis Ababa), recharge identified as being from the plateau seems likely to cross the Ambo fault, whether as ground or surface water. Only in the Mojo catchment is there any evidence for the step-faulting playing an important role. This would explain the plateau-type waters sampled in the Mojo Town area, which according to the ^{14}C evidence are not residual palaeowaters as originally suggested by Craig et al. (1977), but equally cannot be derived simply from the adjacent valley wall because this does not rise beyond 2600 m asl. Recharge of groundwater on the 3000 + m elevations beyond the upper reaches of the Kesem River valley (Fig. 9) appears possible on the assumption that the water is conveyed under confined conditions. This would also explain the existence of plateau-type groundwater in a borehole at the nearby town of Adama (Bretzler et al., 2011), lying within the next sub-catchment down-river. A flowline of ~ 80 km from the recharge area might appear incompatible with the modest residence time inferred from Fig. 6, but simple calculation based on likely values for gradient, permeability and porosity (0.01, 10 m/d and 0.01 respectively) show the possibility of travel times of ~ 100 years, i.e. too young to date reliably by ^{14}C.

Hydrogeological functioning.

Three of the four catchments of the UAB are relatively straightforward in the interpretation of data collected for this study (MK, Mojo and Koka). The fourth, Akaki, is the smallest but most developed as it includes Addis Ababa and its suburbs. However, the higher density of sampling in the Akaki does at least provide the opportunity to define better the hydrogeological features that probably exist to some degree in all four of the catchments.

The Akaki data suggest that hydrogeochemical layering is not prevalent in the catchment. Boreholes sampled towards the top of the catchment range from 92 to 550 m in depth, but according to the stable isotope data all are abstracting a mixture of upper catchment recharge and stream water from the plateau (Fig. 4). Boreholes sampled in the Akaki wellfield range from 140 to 462 m in depth, but each appears to be the product of mixing between lower catchment and stream water from the upper catchment. This extends to site 12 to the NW of the wellfield and (probably) to site 14 in the Koka topographic catchment. To the NE, only the Heineken group (sites 3 – 5) show some vertical layering between overlying upper catchment recharge (3, 4, maximum depth 502 m) and an underlying plateau source (5, at 780 m the deepest sampled borehole in the catchment, with an initial artesian head of 120 m above surface). The Akaki data therefore suggest that downgradient position within the catchment is the most important factor in defining water sources, with intensive abstraction often drawing in waters from neighbouring watercourses, irrespective of borehole depth unless perhaps particularly deep as in the case of site 5 (where confining layers of mudstone and lignite occur at 640–670 and 700–750 m bgl), or if the relief and shape of the catchment bring high ground close to the site, even quite far downgradient as in the case of the Furi extinct volcano a few kilometres N of site 10.

Further evidence for a lack of layering comes from the Mojo catchment, where the group of boreholes around Bishoftu (sites 15, 16, 19–21) have depths ranging from 46–500 m but are all pumping lower catchment recharge, albeit sometimes affected by mixing with evaporated surface water (Figs. 2 and 4).

Renewability.

The rapidly-falling water levels particularly in the Akaki catchment (Hailu et al., 2023) raise the question of how sustainable the ever-increasing yields can be. An approximately 15 km NW–SE transect through the Akaki wellfield (sites 8, 9, 11, 13) and similar UC-LC mixed waters from nearby boreholes (sites 12, 14) offers some evidence (Fig. 10). Despite their different depths, temperatures are very similar (24.4–26.1°C) in all the BHs containing a surface-water component, suggesting a well-mixed water. Likewise, SEC values are similar in all boreholes (503–680 uS/cm). SF_6 modern fractions are low at ≤ 0.03 indicating just a few percent of modern water, but ^{14}C is high in all the surface-water affected boreholes at 76.9–88.1 pmc, showing that the mean residence time of the dominant old water component must be only hundreds rather than thousands of years. While the only borehole

Table 5
Median values for selected minor and trace elements/ions in pumped waters from the four catchments of the Upper Awash Basin. GW – unmixed groundwaters, GW + S – groundwater with surface water component, on isotopic evidence.

Catchment		No. sites	NO_3 mg/L	F mg/L	Si mg/L	Ba µg/L	Sr µg/L	Mn µg/L	Fe_{tot} µg/L	Li µg/L	B µg/L	Co µg/L	Cr µg/L	Cu µg/L	Ni µg/L	Zn µg/L	As µg/L	Se µg/L
Akaki	GW	6	0.19	2.26	41.8	21.9	81	15.7	35.8	55	94	0.014	0.10	2.23	0.13	13.8	4.6	0.09
	GW + S	9	14.1	0.65	32.7	21.5	310	1.3	4.8	15	<50	0.014	1.25	2.04	0.10	3.4	0.45	0.41
Mojo	GW	9	2.87	1.24	51.7	10.8	195	2.3	3.0	38	76	0.115	0.47	1.53	0.21	7.7	2.3	0.36
	GW + S	5	16.6	0.79	38.6	16.6	227	0.9	2.8	13	575	0.078	0.52	2.02	0.60	4.7	2.3	0.37
MK	GW	8	3.40	1.37	51.6	15.4	195	2.6	3.0	34	94	0.072	0.26	1.21	0.15	11.3	2.3	0.38
Koka	GW	1	5.30	0.27	33.0	10.5	514	1.8	1.6	<5	<50	0.009	1.89	3.14	0.29	5.9	0.17	0.19
	GW + S	2	6.47	5.98	45.0	21.0	327	10.6	28.4	67	271	0.048	0.55	1.41	0.31	2.4	1.9	0.46

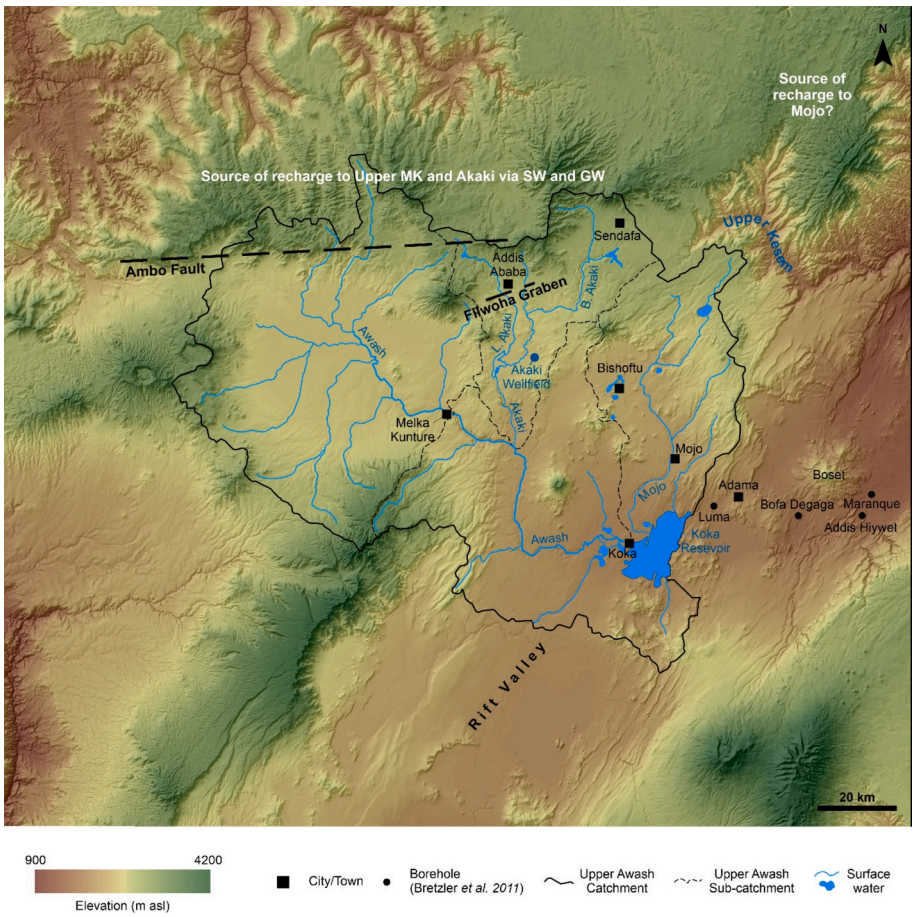

Fig. 9. Terrain map of the Upper Awash basin and adjacent rift valley area, showing the junction between the E–W trending Yerer-Tulu Welel volcanic lineation and the NE–SW trending rift valley with its numerous step faults. These may favour the long-distance transport of plateau recharge to the Mojo wellfield. Also shown are other locations mentioned in the text.

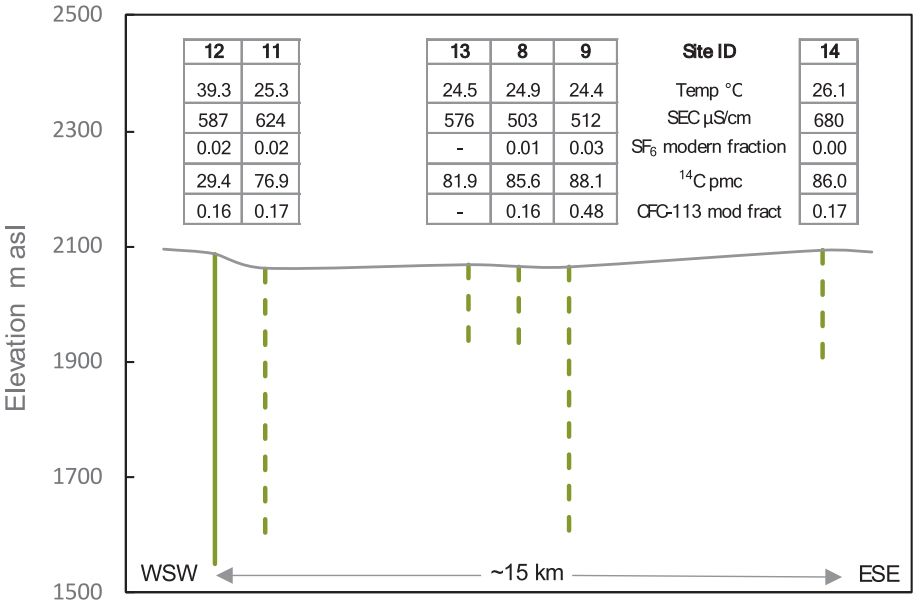

12	11	13	8	9	Site ID	14
39.3	25.3	24.5	24.9	24.4	Temp °C	26.1
587	624	576	503	512	SEC µS/cm	680
0.02	0.02	-	0.01	0.03	SF_6 modern fraction	0.00
29.4	76.9	81.9	85.6	88.1	^{14}C pmc	86.0
0.16	0.17	-	0.16	0.48	CFC-113 mod fract	0.17

Fig. 10. Transect approximately 15 km WSW–ESE through the Akaki wellfield and neighbouring boreholes abstracting mixed upper/lower catchment recharge water (based on $\delta^{18}O$ evidence), with key parameters for each borehole (where measured). Broken lines indicate boreholes with an inferred surface water component.

apparently not affected by surface water (site 12) has a lower ^{14}C activity suggesting the latter, its higher temperature might be an indication of a magmatic input of dead carbon, and its 'real' age might be similar to the others. Indeed, CFC-113 is indicating some wastewater

is entering the groundwater system, including at the supposedly older site 12 (Fig. 5c).

Increased abstraction combined with rapidly falling groundwater levels suggest that an element of non-renewable water use may be occurring, though transition to a new steady-state cannot yet be ruled out (Cuthbert et al., 2024). The abstraction is also capturing new groundwater recharge through ingress from surface water in the longer-established wellfields. At present, the continued depletion of groundwater storage appears to be maintaining the generally good inorganic quality of groundwater in the Akaki catchment, but the rate of change has yet to be determined. Regular monitoring of sensitive indicators like the CFCs would be an effective way to do this.

6.1. Subsurface discharge from the UAB

The basic water balance outlined earlier (2.1) suggests substantial flow of groundwater out of the UAB, indeed the basin is likely to be one of the more important contributors of groundwater to the rift valley (Kebede et al., 2021). In terms of using $\delta^{18}O$ as an environmental tracer, homogenisation of the groundwater at the foot of the basin would be expected on the assumption that the groundwater and surface water catchments coincide at this point.

Subsurface discharge from the UAB has not been investigated by any sampling during the present study, but some evidence exists from previous research. The Koka Dam outlet was measured at –1.5‰ $\delta^{18}O$ and –3‰ $\delta^{2}H$ in November 2007 (Bretzler et al., 2011) but while not obviously affected by evaporation, seems unlikely to represent the isotopic composition of groundwater flow out of the basin, as it is isotopically heavier than much of the groundwater within the basin (Fig. 2). Furthermore, it has been concluded that there is rather little evidence for groundwater–surface water interaction in the rift valley (Kebede et al., 2021), which is predictable in view of the deposits of tephra, silt and clay up to 100 m thick that floor the wider Koka area (Di Paola, 1972). Instead, a bulk stable isotopic value for UAB groundwater would probably lie in the range suggested by Fig. 2b, i.e. ~ –4‰ $\delta^{18}O$, with an $\delta^{2}H$ equivalent of ~ –15‰ based on the Addis Ababa meteoric line from the Global Network of Isotopes in Precipitation (https://nucleus.iaea.org/wiser/indexaspx).

On the basis of local topography, any subsurface flow out of the UAB is likely to be in an ENE direction downgradient of the Koka reservoir. Three sites near Lake Koka were investigated by Bretzler et al. (2011). With $\delta^{18}O$ values of − 3.9 and − 4.7‰, boreholes at Luma and Adama (Fig. 9) are clearly abstracting water originally from higher elevations, but based on medium–high ^{14}C (54.4 pmc) probably from the high ground lying immediately to the north rather than the edge of any outflow plume from the UAB (see also discussion about the Mojo wellfield in 6.1). However, a borehole at Bofa Degaga lying near the centre of the valley to the SE of the town of Adama (Fig. 9) may be more representative. With a $\delta^{18}O$ value of − 3.0‰ and a $\delta^{2}H$ value of –13‰, this apparently unevaporated water could represent UAB outflow mixed with a proportion of inflow from the eastern plateau which appears to yield generally less isotopically-depleted water (Bretzler et al., 2011). Further down the rift valley at Addis Hiywet and Maranque, in the vicinity of the Boset central volcano (Fig. 9), borehole $\delta^{18}O$ values have risen to ~ +0.4‰ suggesting that UAB groundwater flow is no longer readily traceable. However, it may simply be that the boreholes in question are not sufficiently deep to obtain a representative sample of underflow from the UAB; indeed, further down-river at Lake Besaka more-depleted waters occur (Kebede et al., 2008, 2020) which may represent preserved axial flow.

7. Conclusions

The Upper Awash Basin of Ethiopia is a high-relief region where water demand can be locally high, especially in and around the national capital Addis Ababa. Groundwater is increasingly being used to meet this demand, but owing to the mixed volcanic nature of the bedrock a consensus has yet to emerge on the detail of the various aquifer formations present in the basin, and how groundwater is recharged to, and distributed between, these aquifers. Environmental tracers have helped circumvent this: despite little information on borehole construction apart from total depth, combining stable isotopes, trace gases, radiocarbon and hydrochemistry from 40 active boreholes has revealed different facets of how the basin functions hydrogeologically.

A systematic interpretation of stable isotope data has shown the likely elevations of groundwater recharge, and whether waters are likely to be mixed and/or to contain a proportion of surface water. It has been demonstrated that a combination of old and modern residence-time indicators is also essential to understand groundwater behaviour. Water quality has been less diagnostic but has helped to confirm an interpretation of a general lack of layering in the areas sampled via boreholes covering a range of depths. While this does not necessarily invalidate the concept of upper and lower basalt aquifers beneath the UAB, it implies a high degree of hydraulic connectivity exists, conceivably due to intensive exploitation which has increased vertical gradients and mixing. The approach has shown that groundwater mean residence times are largely in the region of hundreds of years rather than thousands, and revealed a significant contribution from surface water bodies. This implies a relatively low storage aquifer where the high abstraction is largely met by recharge, therefore vulnerable to depletion and falling water tables.

The benefits of this particular environmental tracer approach are extendable to other high-relief basins relying heavily on groundwater, from Asia to southern Africa and Latin America. Tracers are especially suitable in mountain environments (Somers and McKenzie 2020 and can provide a rapid initial conceptual model without the need for first undertaking a detailed geological characterisation or waiting decades until sufficient in-situ groundwater monitoring data are available.

CRediT authorship contribution statement

W. George Darling: Writing – original draft, Methodology, Writing – review & editing. **James P.R. Sorensen:** Writing – original draft, Conceptualization, Writing – review & editing, Investigation. **Tilahun Azagegn:** Investigation, Resources, Writing – review & editing. **Behailu Birhanu:** Writing – review & editing, Investigation, Resources. **Seifu Kebede:** . **Daren C. Gooddy:** Resources, Writing – review & editing. **Koos Groen:** Resources, Writing – review & editing. **Richard G. Taylor:** Resources, Conceptualization, Writing – review & editing, Funding acquisition. **Alan M. MacDonald:** Resources, Conceptualization, Writing – review & editing, Writing – original draft, Funding acquisition.

Declaration of competing interest

The authors declare no competing financial interests or personal relationships that could have influenced the work reported in this paper.

Acknowledgments

We thank Taeame Gebremedhin for strong support in the field. Charlotte Vye-Brown provided helpful geological advice. AMM, BB, JPRS, RGT, SK and TA acknowledge GroFutures (Groundwater Futures in Sub-Saharan Africa) via Workpackages NE/M008622/1 and NE/M008932/1. AMM, JPRS and WGD acknowledge TerraFirma Workpackage NE/W004895/1. RGT acknowledges support of CIFAR Fellowship FL-001275. We are grateful to the referees (Prof. Ian Cartwright and two anonymous) for their suggestions on how to improve the manuscript. AMM, DCG, JPRS and WGD contribute with the permission of the Director, British Geological Survey (UKRI).

Data availability

All data used are tabulated in the article

References

Adhana, T.A., 2014. The occurrence of a complete continental rift type of volcanic rocks suite along the Yerer–Tullu Wellel Volcano Tectonic Lineament, Central Ethiopia. J. Afr. Earth Sc. 99, 374–385.

Aeschbach-Hertig, W., Peeters, F., Beyerle, U., Kipfer, R., 2000. Palaeotemperature reconstruction from noble gases in ground water taking into account equilibration with entrapped air. Nature 405, 1040–1044.

Aschale, M., Sileshi, Y., Kelly-Quinn, M., Hailu, D., 2021. Multivariate analysis of potentially toxic elements in surface waters in Ethiopia. Appl. Water Sci. 11, 80. https://doi.org/10.1007/s13201-021-01412-6.

Ayenew, T., Kebede, S., Alemayehu, T., 2008. Environmental isotopes and hydrochemical study applied to surface water and groundwater interaction in the Awash River basin. Hydrol. Process. 22, 1548–1563.

Azagegn, T., Asrat, A., Ayenew, T., Kebede, S., 2015. Litho-structural control on interbasin groundwater transfer in central Ethiopia. J. Afr. Earth Sc. 101, 383–395.

Benvenuti, M., Carnicelli, S., Belluomini, G., Dainelli, N., Di Grazia, S., Ferrari, G.A., Iasio, C., Sagri, M., Ventra, D., Atnafu, B., Kebede, S., 2002. The Ziway–Shala lake basin (main Ethiopian rift, Ethiopia): a revision of basin evolution with special reference to the Late Quaternary. J. Afr. Earth Sc. 35, 247–269.

Berhanu, B., Bisrat, E., 2020. Alleviating water scarcity in the central rift valley lakes through an inter-basin water transfer. Ethiopia. Natural Resources 11, 554.

Berehanu, B., Azagegn, T., Ayenew, T., Masetti, M., 2017. Inter-basin groundwater transfer and multiple approach recharge estimation of the upper Awash aquifer system. Journal of Geoscience and Environment Protection 5, 76. https://doi.org/10.4236/gep.2017.53007.

Birhanu, B., Kebede, S., Charles, K., Taye, M., Atlaw, A., Birhane, M., 2021. Impact of natural and anthropogenic stresses on surface and groundwater supply sources of the upper Awash sub-basin. Central Ethiopia. Frontiers in Earth Science 9, 656726.

Bonini, M., Corti, G., Innocenti, F., Manetti, P., Mazzarini, F., Abebe, T., Pecskay, Z., 2005. Evolution of the Main Ethiopian Rift in the frame of Afar and Kenya rifts propagation. Tectonics 24, TC1007. https://doi.org/10.1029/2004TC001680.

Bretzler, A., Osenbrück, K., Gloaguen, R., Ruprecht, J.S., Kebede, S., Stadler, S., 2011. Groundwater origin and flow dynamics in active rift systems–a multi-isotope approach in the Main Ethiopian Rift. J. Hydrol. 402, 274–289.

Cartwright, I., Currell, M.J., Cendon, D.I., Meredith, K.T., 2020. A review of the use of radiocarbon to estimate groundwater residence times in semi-arid and arid areas. J. Hydrol. 580, 124247.

Chan, W.C., Thompson, J.R., Taylor, R.G., Nay, A.E., Ayenew, T., MacDonald, A.M., Todd, M.C., 2020. Uncertainty assessment in river flow projections for Ethiopia's Upper Awash Basin using multiple GCMs and hydrological models. Hydrol. Sci. J. 65, 1720–1737. https://doi.org/10.1080/02626667.2020.1767782.

Clark, I.D., Fritz, P., 1997. Environmental Isotopes in Hydrogeology. CRC Press, Boca Raton, p. 343.

Craig, H., Lupton, J. and Horowitz, R., 1977. Isotopic Geochemistry and Hydrology of Geothermal Waters in the Ethiopian Rift Valley, Rep. 77-14, Scripps Inst. Oceanogr.

Cuthbert, M.O., Gleeson, T., Bierkens, M.F.P., Ferguson, G., Taylor, R.G., 2024. Concerns regarding proposed groundwater Earth system boundary. Nature 635, E4–E5.

Daba, M.H., Ayele, G.T., You, S., 2020. Long-Term Homogeneity and Trends of Hydroclimatic Variables in Upper Awash River Basin. Ethiopia. Advances in Meteorology 2020. https://doi.org/10.1155/2020/8861959.

Darling, W.G., 1998. Hydrothermal hydrocarbon gases: 2, Application in the East African Rift system. Appl. Geochem. 13, 825–840.

Darling, W.G., Gizaw, B., Arusei, M.K., 1996. Lake-groundwater relationships and fluid-rock interaction in the East African Rift Valley: isotopic evidence. J. Afr. Earth Sc. 22, 423–431.

Darling, W.G., Gooddy, D.C., MacDonald, A.M., Morris, B.L., 2012. The practicalities of using CFCs and SF_6 for groundwater dating and tracing. Appl. Geochem. 27, 1688–1697.

Demlie, M., Wohnlich, S., Wisotzky, F., Gizaw, B., 2007. Groundwater recharge, flow and hydrogeochemical evolution in a complex volcanic aquifer system, central Ethiopia. Hydrgeol. J. 15, 1169–1181.

Demlie, M., Wohnlich, S., 2006. Soil and groundwater pollution of an urban catchment by trace metals: case study of the Addis Ababa region, central Ethiopia. Environ. Geol. 51, 421–431.

Demlie, M., Wohnlich, S., Ayenew, T., 2008. Major ion hydrochemistry and environmental isotope signatures as a tool in assessing groundwater occurrence and its dynamics in a fractured volcanic aquifer system located within a heavily urbanized catchment, central Ethiopia. J. Hydrol. 353, 175–188.

Demlie, M., 2015. Assessment and estimation of groundwater recharge for a catchment located in highland tropical climate in central Ethiopia using catchment soil–water balance (SWB) and chloride mass balance (CMB) techniques. Environ. Earth Sci. 74, 1137–1150.

Di Paola, G.M., 1972. The Ethiopian Rift Valley (between 7 00′ and 8 40′ lat. north). Bull. Volcanol. 36, 517–560.

Edmunds, W.M., 2008. Groundwater in Africa – Palaeowater, climate change and modern recharge. In: Applied Groundwater Studies in Africa. CRC Press, pp. 315–332.

Eshetu, Z., Högberg, P., 2000. Reconstruction of forest site history in Ethiopian highlands based on ^{13}C natural abundance of soils. AMBIO J. Hum. Environ. 29, 83–89.

Fulda, C., Kinzelbach, W., 2000. Sulphur Hexafluoride (SF6) as a New Age-Dating Tool for Shallow Groundwater: Methods and First Results. IAHS Publication No.262. IAHS Press, Wallingford, Oxfordshire, UK.

Gat, J.R., 1971. Comments on the stable isotope method in regional groundwater investigations. Water Resour. Res. 7, 980–993.

Gelaye, Y., 2023. The status and natural impact of floriculture production in Ethiopia: a systematic review. Environ. Sci. Pollut. Res. 30, 9066–9081.

Gonfiantini, R., Roche, M.A., Olivry, J.C., Fontes, J.C., Zuppi, G.M., 2001. The altitude effect on the isotopic composition of tropical rains. Chem. Geol. 181, 147–167.

Gustard, A., Bullock, A., Dixon, J. M.. 1992. Low flow estimation in the United Kingdom. Wallingford, Institute of Hydrology, 88pp. (IH Report No.108).

Hailu, K., Birhanu, B., Azagegn, T., Kebede, S., 2023. Regional groundwater flow system characterization of volcanic aquifers in upper Awash using multiple approaches, central Ethiopia. Isot. Environ. Health Stud. https://doi.org/10.1080/10256016.2023.2222221.

Han, L.F., Wassenaar, L.I., 2021. Principles and uncertainties of ^{14}C age estimations for groundwater transport and resource evaluation. Isot. Environ. Health Stud. 57, 111–141.

Jasechko, S., Perrone, D., Befus, K.M., Bayani Cardenas, M., Ferguson, G., Gleeson, T., Luijendijk, E., McDonnell, J.J., Taylor, R.G., Wada, Y., Kirchner, J.W., 2017. Global aquifers dominated by fossil groundwaters but wells vulnerable to modern contamination. Nat. Geosci. 10, 425–429.

Jasechko, S., Seybold, H., Perrone, D., Fan, Y., Shamsudduha, M., Taylor, R.G., Fallatah, O., Kirchner, J.W., 2024. Rapid groundwater decline and some cases of recovery in aquifers globally. Nature 625, 715–721.

Kebede, S., Travi, Y., 2012. Origin of the $\delta^{18}O$ and $\delta^{2}H$ composition of meteoric waters in Ethiopia. Quat. Int. 257, 4–12.

Kebede, S., Ayenew, T., Umer, M., 2001. Application of isotope and water balance approaches for the study of the hydrogeological regime of the Bishoftu crater lakes. Ethiopia. SINET: Ethiopian Journal of Science 24, 151–166.

Kebede, S., Travi, Y., Asrat, A., Alemayehu, T., Ayenew, T., Tessema, Z., 2008. Groundwater origin and flow along selected transects in Ethiopian rift volcanic aquifers. Hydrgeol. J. 16, 55–73.

Kebede, S., Travi, Y., Stadler, S., 2010. Groundwaters of the Central Ethiopian Rift: diagnostic trends in trace elements, $\delta^{18}O$ and major elements. Environ. Earth Sci. 61, 1641–1655.

Kebede, S., Charles, K., Godfrey, S., MacDonald, A., Taylor, R.G., 2021. Regional-scale interactions between groundwater and surface water under changing aridity: evidence from the River Awash Basin, Ethiopia. Hydrol. Sci. J. 66, 450–463.

Lemma, B., Kebede Gurmessa, S., Nemomissa, S., Otte, I., Glaser, B., Zech, M., 2020. Spatial and temporal ^{2}H and ^{18}O isotope variation of contemporary precipitation in the Bale Mountains, Ethiopia. Isot. Environ. Health Stud. 56, 122–135.

MacDonald, A.M., Lark, R.M., Taylor, R.G., Abiye, T., Fallas, H.C., Favreau, G., Goni, I.B., Kebede, S., Scanlon, B., Sorensen, J.P., Tijani, M., 2021. Mapping groundwater recharge in Africa from ground observations and implications for water security. Environ. Res. Lett. 16, 034012.

McCallum, J.L., Cook, P.G., Simmons, C.T., 2015. Limitations of the use of environmental tracers to infer groundwater age. Groundwater 53, 56–70.

McKenzie, J.M., Mark, B.G., Thompson, L.G., Schotterer, U., Lin, P.N., 2010. A hydrogeochemical survey of Kilimanjaro (Tanzania): implications for water sources and ages. Hydrgeol. J. 18, 985–995.

Muleta, D., Abate, B., 2021. Groundwater hydrodynamics and sustainability of Addis Ababa city aquifer. Groundw. Sustain. Dev. 12, 100485. https://doi.org/10.1016/j.gsd.2020.100485.

Otte, I., Detsch, F., Gütlein, A., Scholl, M., Kiese, R., Appelhans, T., Nauss, T., 2017. Seasonality of stable isotope composition of atmospheric water input at the southern slopes of Mt. Kilimanjaro. Tanzania. Hydrological Processes 31, 3932–3947.

Pearson Jr, F.J., Hanshaw, B.B., 1970. Sources of dissolved carbonate species in ground water and their effects on carbon-14 dating. In Isotope Hydrology 1970, 1–26.

Rodell, M., Famiglietti, J.S., Wiese, D.N., Reager, J.T., Beaudoing, H.K., Landerer, F.W., Lo, M.H., 2018. Emerging trends in global freshwater availability. Nature 557, 651–659.

Scanlon, B.R., Rateb, A., Anyamba, A., Kebede, S., MacDonald, A.M., Shamsudduha, M., Small, J., Sun, A., Taylor, R.G., Xie, H., 2022. Linkages between GRACE water storage, hydrologic extremes, and climate teleconnections in major african aquifers. Environ. Res. Lett. 17, 014046.

Scanlon, B.R., Fakhreddine, S., Rateb, A., de Graaf, I., Famiglietti, J., Gleeson, T., Grafton, R.Q., Jobbagy, E., Kebede, S., Kolusu, S.R., Konikow, L.F., 2023. Global water resources and the role of groundwater in a resilient water future. Nature Reviews Earth & Environment 4, 87–101.

Somers, L.D., McKenzie, J.M., 2020. A review of groundwater in high mountain environments. Wiley Interdiscip. Rev. Water 7, e1475.

Tadesse, E., Azagegn, T. and Alemayehu, T., 2023. Characterizing groundwater and surface water interaction using geological, environmental tracers (^{222}Rn, EC, $\delta^{18}O$, and $\delta^{2}H$) and baseflow index methods for part of the Upper Awash and the adjacent Blue Nile Basin, Ethiopia. Journal of African –Earth Sciences, p.104992. https://doi.org/10.1016/j.jafrearsci.2023.104992.

Tafesse, J., 2018. Comparative evaluation of shallow groundwater dynamics of Becho and Koka Plains. MSc thesis, Univ. Addis Ababa, 94pp.

Tarekegn, M.M., Weldekidan, G.L., 2022. Concentration Levels of Heavy Metals and selected Ions in the Irrigation Water: the Case of Little Akaki River, Addis Ababa, Ethiopia. In: Salah, H.M., Hassan, A.I. (Eds.), Chaper 8 in Environmental Impact and Remediation of Heavy Metals.

Tekleab, S., Wenninger, J., Uhlenbrook, S., 2014. Characterisation of stable isotopes to identify residence times and runoff components in two meso-scale catchments in the Abay/Upper Blue Nile basin, Ethiopia. Hydrol. Earth Syst. Sci. 18, 2415–2431.

Thaw, M., Visser, A., Rungee, J., Oerter, E.J., Conklin, M., 2025. Water stable isotopes in precipitation, rivers, and groundwater across an elevation gradient in the Sierra Nevada Mountains (USA) reflect source elevation. Hydrol. Processes 39, e70177.
Tolera, M.B., Chung, I.M., Chang, S.W., 2018. Evaluation of the climate forecast system reanalysis weather data for watershed modeling in Upper Awash basin. Ethiopia. Water 10, 725.
USGS, 2022. Website https://water.usgs.gov/lab/software/air_curve/ accessed February 2022.
Yimer, Y.A., Geberkidan, A., 2020. The pollution status of Awash River Basin (Ethiopia) using descriptive statistical techniques. American Journal of Water Resources 8, 56–68.
Yitbarek, A., Razack, M., Ayenew, T., Zemedagegnehu, E., Azagegn, T., 2012. Hydrogeological and hydrochemical framework of Upper Awash River basin, Ethiopia: with special emphasis on inter-basins groundwater transfer between Blue Nile and Awash Rivers. J. Afr. Earth Sc. 65, 46–60.
Zuber, A. and Małoszewski, P., 2001. 2 - Lumped parameter models. Environmental isotopes in the hydrological cycle: Principles and applications, pp.5-35.